Stochastic Environmental Research and Risk Assessment
https://doi.org/10.1007/s00477-024-02786-0

ORIGINAL PAPER

# Evaluating changes in flood frequency due to climate change in the Western Cape, South Africa

**Kamleshan Pillay**[1] · **Mulala Danny Simatele**[1]

Accepted: 16 July 2024


**Abstract**
This study assesses the impact of climate change on flood frequency across seven sites in the Western Cape province of South Africa. The calibrated Water Resources Simulation Model (WRSM)/Pitman hydrological model was run using precipitation inputs from two representative concentration pathways (RCP) scenarios (RCP 4.5 and 8.5) using a combination of eight global circulatory models (GCM) for the two periods (2030–2060 and 2070–2100). GCMs were statistically downscaled using the delta change (DC), linear scaling (LS) and quantile delta mapping (QDM) approaches. Average daily discharge was estimated from each downscaled daily precipitation dataset using the Pitman/WRSM model with the Fuller and Sangal estimation methods used to calculate daily instantaneous peak flows. Flood frequency curves (FFC) were generated using the annual maximum series (AMS) for the GCM ensemble mean and individual GCMs for the return periods between 2 and 100 years. FFCs generated based on LS and QDM downscaling methods were aligned for the GCM ensemble mean in terms of the direction of FFCs. Further analysis was conducted using outputs based on the QDM approach, given its suitability in projecting peak flows. Under this method, both Fuller and Sangal FFCs exhibited a decreasing trend across the Jonkershoek and Little Berg River sites; however, estimated quantiles for low-probability events were higher under the Fuller method. This study noted the variation in FFCs from individual GCMs compared to the FFC representing the GCM ensemble mean. Further research on climate change flood frequency analysis (FFA) in South Africa should incorporate other advanced downscaling and instantaneous peak flow estimation (IPF) methods.

**Keywords** Climate change · Extreme weather · Floods · Flood frequency analysis · South Africa · Western Cape

## 1 Introduction

Flooding is the most common natural hazard globally, causing significant loss of life and destruction of property and infrastructure. Between 2000 and 2022, floods worldwide resulted in inflation-adjusted economic losses equivalent to US $ 929 billion, representing 3852 floods (Centre for Research on the Epidemiology of Disasters (CRED) 2023). Storms and flooding events are the most common types of natural hazards in South Africa, constituting 71.2% of the total hazards in the country (CRED 2023). In the Western Cape, flooding is driven primarily by cut-off lows, resulting in persistent annual financial losses across the province. Between 2003 and 2014, government departments and municipalities in the province experienced ZAR 4.9 billion in flood-related damages (Pharoah et al. 2016).

Flood frequency analysis (FFA) is used to estimate flood magnitudes associated with specific return periods beyond the observed record (Cunnane 1988). FFA is referred to as design flood estimation. The understanding of the magnitudes of floods and their exceedance probabilities is of prime importance for various aspects of water resources management and planning such as the design of hydraulic structures (Smithers et al. 2015), flood insurance studies (Kjeldsen et al. 2014), flood plain management (Nagy et al. 2017), river ecological studies (Zaman et al. 2012), and stormwater management (Leščešen et al. 2019). FFA faces several challenges in its implementation, with issues such as the selection of theoretical probability distributions and the short record length of gauge data being particularly problematic (Nagy et al. 2017).

✉ Kamleshan Pillay
pillay.kamleshan@gmail.com

[1] School of Geography, Archaeology and Environmental Studies 1 Jan Smuts Avenue, Braamfontein 2000, Johannesburg, South Africa

Published online: 30 July 2024

FFA can be undertaken at the site or regional level. At the site level, FFA is the most direct method of estimating design floods (Zaman et al. 2012) and uses a record of observed flows at a specific location. Regional FFA refers to the assessment of magnitudes of peak flows at sites clustered as homogenous flood regions owing to similar at-site characteristics (Hosking and Wallis 1997). Regional FFA approaches are advantageous in overcoming issues such as short record lengths and the spatial density of river gauges. At-site FFA is usually undertaken on gauged flow data at a given location if flow data are available for the site under investigation.

FFA can be undertaken using the AMS or partial duration series (PDS). AMS is derived from the highest peak discharge value for each year in the time series (Langbein 1949). The AMS approach is advantageous as events are easily identified, and the approach ensures that selected events are independent of each other. The AMS approach can ignore larger peaks that are not the maximum in their years and be problematic in semi-arid and arid regions where annual peaks can be low (Zaman et al. 2012). In contrast, the PDS approach includes all flood events over a predefined level for each year. The PDS approach is suitable when time series records are short and less reliable (Nagy et al. 2017). The PDS method is limited by its ability to ensure the independence of the flood peaks and the absence of a standardised approach for the selection of appropriate threshold values. In South African studies, observed flows are usually fitted to the AMS extracted from the discharge series (Nathanael et al. 2018; Ngongondo et al. 2013; Singo et al. 2016; Smithers et al. 2015; Kjeldsen et al. 2002).

There is no one theoretical probability distribution that applies to all sites, with most research suggesting that distributions be selected based on goodness of fit tests (Markiewicz et al. 2015). In South Africa, the most common probability distributions used in FFA are the Log-Normal (LN), Log Pearson Type III (LP3) and Generalized Extreme Value (GEV) distributions (Van der Spuy and du Plessis 2022). Despite concerns regarding the length and reliability of discharge series records in South Africa, the GEV and LP3 distributions generally produce acceptable results (Van der Spuy and du Plessis 2022).

Precipitation across South Africa is highly variable (MacKellar et al. 2014). While rainfall climate projections remain uncertain, the majority of climate models suggest that annual rainfall will decline across the country (World Bank Group 2021). Despite decreases in average precipitation, rainfall intensity is expected to increase under future climate scenarios in South Africa (Abiodun et al. 2020; Kruger and Nxumalo 2017; Engelbrecht et al. 2013; Westra et al. 2013). Intense rainfall is the primary driver of floods in South Africa in smaller catchments compared to widespread rainfall in larger catchments (Smithers and Schulze 2004). Therefore, with the projected increase in rainfall intensity, the prevalence of flooding will likely increase across the region.

The Western Cape province of South Africa experiences Mediterranean winter rainfall due to the influence of mid-latitude cyclones (du Plessis and Schloms 2017; Roffe et al. 2019). Winter rainfall in parts of the Western Cape of South Africa is expected to decline due to climate change (Engelbrecht et al. 2013). Synoptic features which drive extreme weather events such as floods are potentially increasing in the Western Cape (Engelbrecht et al. 2013; Abiodun et al. 2016). Pharoah et al. (2016) note that extreme daily cut-off low-induced rainfall has increased across the Western Cape province, coupled with record flood peaks in several rivers between 2003 and 2014. De Waal et al. (2017) show that 63% of rainfall stations in the Western Cape exhibited an increase in 20- and 50-year, 1-day rainfall extremes.

Numerous studies have been conducted on the linkage of climate change to flood frequency (Dong et al. 2018; Iqbal et al. 2018; Maurer et al. 2018; Quintero et al. 2018; Almasi and Soltani 2017; Camici et al. 2014; Qin and Lu 2014; Shaw and Riha 2011; Mareuil et al. 2007; Kay et al. 2006; Muzik 2002). In the South African context, traditional FFA studies have been undertaken in several provinces, including KwaZulu-Natal (Kjeldsen et al. 2002); Mpumalanga (Heritage et al. 2001); Limpopo (Singo et al. 2016); and the Western Cape (Tempelhoff et al. 2009). However, few studies have focused on flood frequency estimation under future climate change scenarios in South Africa. Studies undertaken by Abiodun et al. (2020), Du Plessis and Scholms (2017), and De Waal et al. (2017) have focused on flood design estimations based on extreme rainfall under future climate change in the Western Cape; however, no studies have been undertaken using discharge series from river gauges across the province.

The assessment of flood frequency as a result of climate change is typically assessed using global circulation models (GCMs), downscaling techniques, and hydrological models (Xu et al. 2005). The coarse resolution of GCMs (approximately 150–300 $km^2$) cannot serve as direct inputs into hydrological models (Ougahi et al. 2022). Therefore, downscaling techniques must be applied to GCMs to obtain a finer spatial or temporal resolution (Dong et al. 2018; Iqbal et al. 2018; Maurer et al. 2018; Quintero et al. 2018; Almasi and Soltani 2017; Camici et al. 2014; Qin and Lu 2014). There are two primary categories of downscaling: dynamical downscaling and statistical downscaling. In dynamical downscaling, a high-resolution climate model (a regional climate model (RCM)) that is limited to a specific region is run using one or more GCM grids, with the boundary conditions driven by the underlying GCM (Seidou et al. 2012). RCMs provide outputs at a finer solution resolution (20–60 $km^2$, compared to GCMs (150–300 $km^2$) (Chokkavarapu and

Mandla 2019). Statistical downscaling refers to the statistical relationship that is developed between historical observational data and outputs of climate models (both regional and global) (Copernicus Climate Change Service 2021). This study is limited to statistical downscaling methods as these approaches are computationally inexpensive. In addition, statistical downscaling methods are helpful in downscaling to point locations, such as a weather station or river gauge.

This paper examines the changes in flood frequency curves (FFC) across selected sites in the Western Cape province in South Africa. The specific objectives of the study include:

- Evaluating FFCs under three statistical downscaling methods (delta change (DC), linear scaling (LS) and quantile delta mapping (QDM) approaches) and two instantaneous peak flow (IPF) estimation methods: the Sangal and Fuller methods.
- Comparing FFCs generated between individual GCMs and the GCM ensemble mean FFC.
- Investigating changes in FFCs under future climate scenarios (representative concentration pathway (RCP) 4.5 and RCP 8.5) for two periods (2030–2060 and 2070–2100).

## 2 Methodology

### 2.1 Study area

The Western Cape province is situated in the southwestern corner of South Africa and is one of the country's nine provinces (Fig. 1). The province is bordered by the Eastern Cape and Northern Cape provinces. The Western Cape has a total area of 129 462 km$^2$ and is characterised by a semi-arid climate with an annual average rainfall of 450 mm with significant variability across the province (Western Cape Government 2018). The Western Cape comprises two water management areas (WMA): the Breede-Gouritz and the Berg-Olifants (Western Cape Government 2018).

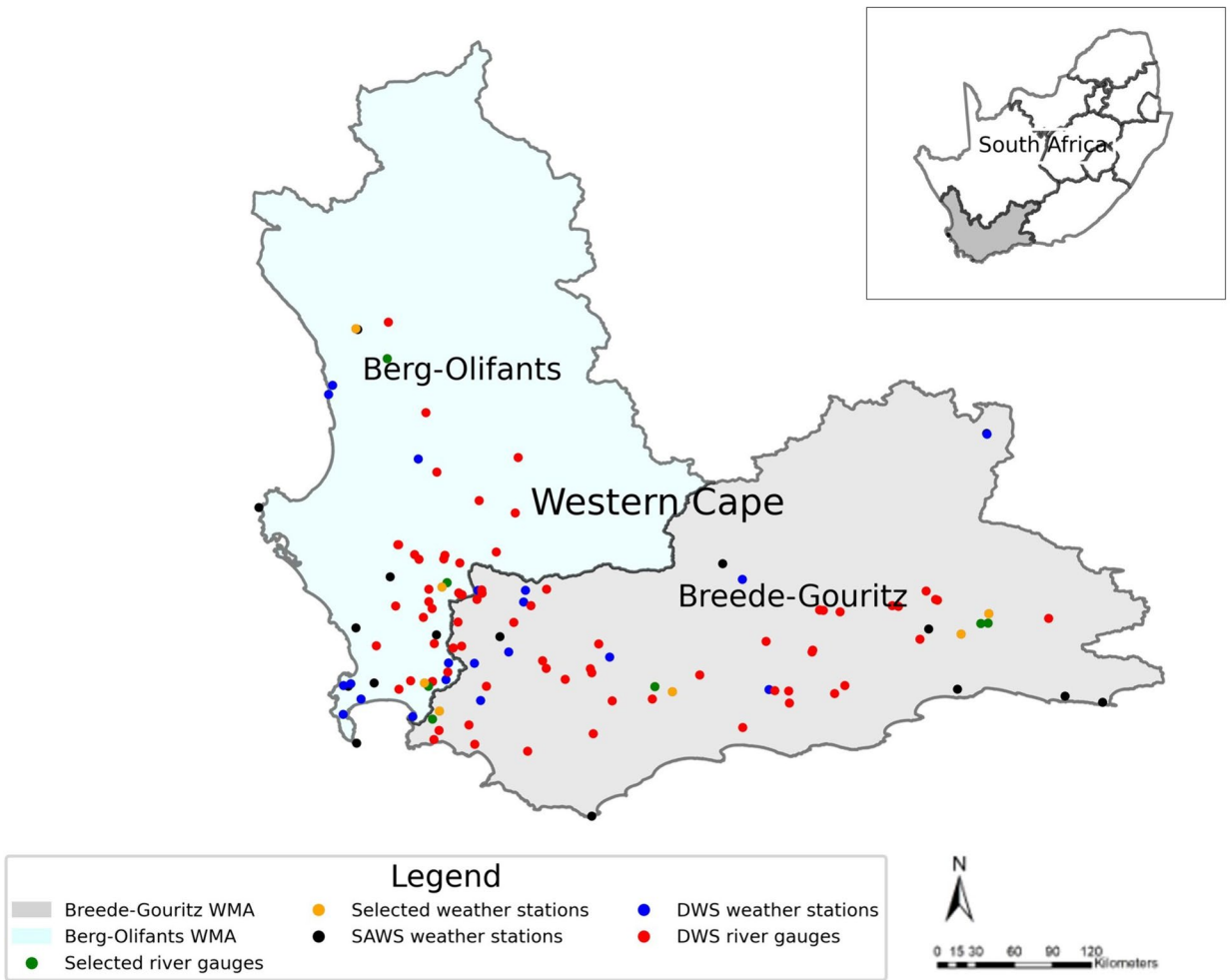


**Fig. 1** Map of the Western Cape province illustrating selected river gauges and weather stations across water management areas

## 2.2 Data acquisition

Daily precipitation data was acquired from the South African Weather Service (SAWS) climate database and the hydrological services platform of the Department of Water and Sanitation (DWS). Average daily discharge and monthly evaporation data were obtained from the hydrological services platform of the Department of Water and Sanitation. Rainfall stations and river gauges were assessed to ensure a sufficiently long data record was present. To ensure consistency across sites, the data period of 1970–2000 was selected. Data completeness was evaluated for each river gauge and rainfall station. The proportion of missing observations was less than 1% on average across all sites. Missing data was interpolated using the Kalman smoothing function which is recommended for long time series correction (Moritz 2017). This was undertaken using the R-based ImputeTS package. This approach has been applied successfully in other studies focused on flood frequency and precipitation changes under future climate change (Bulti et al. 2021; Brönnimann et al. 2019; Ngongondo et al. 2011). The location of precipitation stations and river gauges are detailed in Tables 1 and 2, and As precipitation stations and river gauges seldom occur in the same geographical location, pairs of precipitation stations and river gauges were matched based on a least distance criterion. In addition, pairs were assessed to ensure their joint presence in the tertiary and quaternary catchments and similarity with respect to biophysical variables such as topography and climate. SAWS data sets are available upon request at https://www.weathersa.co.za/home/equiries_climatedata, while DWS datasets can be downloaded from https://www.dws.gov.za/Hydrology/Verified/hymain.aspx.

## 2.3 GCM acquisition and clustering, scenario selection and downscaling

Climate projections used within this study were based on eight GCMs of the World Climate Research Project Coupled Model Intercomparison Project—Phase 5 (CMIP5) (Table 3). Suitable GCMs were identified using the GCMeval tool developed by Parding et al. (2020). The tool was used to rank, contrast and filter CMIP5 climate models that best represent present precipitation trends in the Southern Africa region while considering bias, spatial correlation and other skill scores. In addition to the models selected using the GCMeval tool, this study integrated two additional climate models (MIROC5 and GFDL-ESM2G) into the ensemble in order to be consistent with a prior investigation conducted in the same location by Pillay (2023). The CMIP5 data was downloaded from the Earth System Grid Federation platform (https://esgf-node.llnl.gov/projects/esgf-llnl/). For all GCMs, historical precipitation data from 1961 to 2005 and future-projected precipitation data from 2006 to 2100 under RCP 4.5 and RCP 8.5 scenarios were acquired.

Raw GCMs must be downscaled to be viable for applications at a local scale. Three statistical downscaling

**Table 1** Summary of rainfall station locations and characteristics

| Rainfall station | Data period | Data source | Latitude (Decimal Degrees) | Longitude (Decimal Degrees) | River Catchment |
|---|---|---|---|---|---|
| Vredendal | 1958–2022 | DWS | – 31.667 | 18.483 | Berg-Olifants |
| Jonkershoek | 1968–2022 | DWS | – 33.964 | 18.929 | Berg-Olifants |
| Vogel Vallij | 1952–2022 | DWS | – 33.342 | 19.041 | Berg-Olifants |
| Grabouw | 1970–2021 | SAWS | – 34.145 | 19.024 | Berg-Olifants |
| Eenzaamheid | 1969–2022 | DWS | – 34.020 | 20.536 | Breede-Gouritz |
| Stompdrift Dam | 1968–2022 | DWS | – 33.513 | 22.587 | Breede-Gouritz |
| Kammanassie | 1926–2022 | DWS | – 33.646 | 22.408 | Breede-Gouritz |

**Table 2** Summary of river gauge locations and characteristics

| River Gauge | River Catchment | Catchment size ($km^2$) | Data period | River Gauge latitude | River Gauge longitude |
|---|---|---|---|---|---|
| Doring River | Berg-Olifants | 24 044 | 1908–2022 | – 31.863 | 18.686 |
| Jonkershoek | Berg-Olifants | 24 | 1998–2022 | – 34.003 | 18.763 |
| Little Berg River | Berg-Olifants | 393 | 1954–2022 | – 33.314 | 19.075 |
| Palmiet | Berg-Olifants | 147 | 1957–2022 | – 34.197 | 18.981 |
| Hermitage | Breede-Gouritz | 9 | 1960–2022 | – 33.987 | 20.422 |
| Marnewicks River | Breede-Gouritz | 23 | 1990–2022 | – 33.576 | 22.582 |
| Vermaaks River | Breede-Gouritz | 22 | 1990–2022 | – 33.578 | 22.535 |

**Table 3** Description of the CMIP5 climate models used (CEDA 2024)

| Model | Institution | Spatial resolution (Lon × Lat) |
|---|---|---|
| CanESM2 | Canadian Centre for Climate Modelling and Analysis of Environment and Climate Change Canada | 2.81 × 2.81 |
| CNRM-CM5 | Centre National de Recherches Meteorologiques (CNRM) and Centre European de Recherches et de Formation Avancee en Calcul Scientifique (CERFACS) | 1.41 × 1.41 |
| GFDL-ESM2G | Geophysical Fluid Dynamics Laboratory (GFDL) | 2.5 × 2.0 |
| MIROC5 | Atmosphere and Ocean Research Institute (AORI), Centre for Climate System Research—National Institute for Environmental Studies (CCSR-NIES), Japan Agency for Marine-Earth Science and Technology (JAMSTEC) | 1.41 × 1.41 |
| MIROC-ESM | Atmosphere and Ocean Research Institute (AORI), Centre for Climate System Research—National Institute for Environmental Studies (CCSR-NIES), Japan Agency for Marine-Earth Science and Technology (JAMSTEC) | 2.81 × 2.81 |
| MRI-CGCM-3 | Meteorological Research Institute of the Japan Meteorological Agency | 1.13 × 1.13 |
| ACCESS1-0 | Commonwealth Scientific and Industrial Research Organization and Bureau of Meteorology (BOM) | 1.88 × 1.25 |
| CMCC-CMS | Centro Euro-Mediterraneo per I Cambiamenti Climatici Climate Model CMCC-CM | 1.88 × 1.88 |

methods were applied in this study. These include the DC, LS and QDM methods. The control period for statistical downscaling was 1970–2000, while the future periods under investigation were 2030–2060 and 2070–2100. The DC and LS approaches are described by Eqs. 1 and 2.

$$P_{DC} = P_{obs,d} \times \frac{\mu\left(P_{sim,m}\right)}{\mu\left(P_{hst,m}\right)} \tag{1}$$

$$P_{LS} = P_{sim,d} \times \frac{\mu\left(P_{obs,m}\right)}{\mu\left(P_{hst,m}\right)} \tag{2}$$

where $P$ is precipitation, *obs* is the observed time series, *hst* is the GCM output of the control period, and *sim* refers to the GCM output of future scenarios. $\mu$ refers to the mean, while $m$ and $d$ refer to the monthly and daily time step.

The QDM approach differs from the DC and LS techniques as it allows the climate change trend to be extracted from projected quantiles. This is advantageous as it allows for quantile corrections across the full distribution of values, thereby matching the reference distribution (Camici et al. 2014). As Xavier et al. (2022, p. 178) outlined, the QDM approach "preserves model-projected relative changes in precipitation data, and it corrects possible systematic biases in the quantiles of modelled data in respect to observed values." The QDM implementation is broken down into two steps. First, the absolute or relative changes in the quantiles between the reference and future periods are calculated. This is represented by Eq. 3. Thereafter, the bias-corrected precipitation dataset is attained by multiplying the relative changes by the historical corrected value—Eq. 4. Further details on the QDM are outlined in Cannon et al. (2015).

$$\Delta_{sim}(i) = \frac{Q_{sim(i)}}{F_{hst}^{-1}\left[F_{sim}\left[Q_{sim(i)}\right]\right]} \tag{3}$$

$$P_{QDM} = F_{obs}^{-1}\left[F_{sim}\left[Q_{sim(i)}\right]\right] \times \Delta_{sim}(i) \tag{4}$$

where $\Delta sim\ (i)$ is the relative changes in the $i$th quantiles between historical and future GCM simulation, and $Qsim(i)$ is the $i$th quantile of future simulated data. $Fsim$ and $Fhst^{-1}$ represent the cumulative distribution function (CDF) for the future period and the inverse CDF of the simulated historical period, respectively.

## 2.4 Hydrological modelling

### 2.4.1 Overview of the water resources simulation model (WRSM)/pitman daily time step model

The WRSM/Pitman daily time step model was used to simulate future average daily discharge estimates. The WRSM/Pitman model is a mathematical model that tracks water movement through a network of catchments, irrigation areas, reservoirs, mining activities and river channels (Bailey and Pitman 2016). The mathematical framework of the model was initially developed and communicated in Pitman (1976). The mathematical model was coded and run in Python 3.11. Daily precipitation and monthly evaporation were inputs to the WRSM/Pitman model. Mean daily evaporation estimates were derived from monthly evaporation estimates.

The WRSM/Pitman model is advantageous for the simulation of future average daily discharge data as less uncertainty is introduced into the modelling framework owing to fewer input data requirements. Hydrological simulations for future climate change scenarios were performed using the

parameters estimated based on the historical calibrations of observed and simulated average daily discharge for the control period (1970–2000).

#### 2.4.2 Mathematical framework

The WRSM/Pitman daily time step model initially disaggregated daily precipitation into hourly intervals. The mathematical relationship between hourly and daily rainfall amounts was assessed using data from weather stations in Pretoria in the Gauteng province (Pitman 1976). Equation 5 was used to determine the storm event duration in hours, while Eq. 6 was used to calculate the hourly precipitation amounts and was based on a typical S-shaped rainfall mass curve. Evaporation and interception losses were removed from hourly precipitation amounts, with the remaining daily precipitation available for surface runoff or infiltration. Surface runoff was calculated using a symmetrical triangular frequency distribution and is described in Eqs. 7–12 with the remaining water available as soil moisture. Soil moisture percolates into groundwater before entering the river channel. These processes are described in Eqs. 13 and 14. Lastly, total discharge was calculated by adding groundwater outflow and surface water runoff while accounting for time delays and attenuation using the Muskingum method.

$$d = 0.964 + 0.13736 \times p \tag{5}$$

$$y = \frac{x^n}{x^n + (1-x)^n} \tag{6}$$

where $y$ is the cumulative precipitation for the event duration (mm) divided by total precipitation (mm per event), $x$ is the cumulative time (hours) divided by total event time (hours), $n$ = exponent related to the non-uniformity of precipitation input (mm), $d$ represents the duration of a storm event (hours), and $p$ is the precipitation (mm/day).

$$R_h = \frac{2(P_h - Z1)^3}{3(Z3 - Z1)^2}; \quad Z1 \le P_h \le Z2 \tag{7}$$

$$R_h = P_h - Z2 + \frac{2\left(P_h - Z1\right)^3}{3(Z3 - Z1)^2}; \quad Z2 \le P_h \le Z3 \tag{8}$$

$$R_h = P_h - Z2; \quad P_h \ge Z3 \tag{9}$$

$$Z1 = \frac{Z_{min} Z3}{Z_{max}} \tag{10}$$

$$Z2 = \frac{(Z1 + Z3)}{2} \tag{11}$$

$$Z3 = \frac{4Z_{max}}{2^{\frac{2S}{St}}} \tag{12}$$

where $P_h$ is hourly rainfall (mm/h), $R_h$ is the surface runoff (mm/h), $Z_{min}$ is the nominal minimum infiltration rate (mm/h), $Z_{max}$ is the nominal maximum infiltration rate (mm/h), $S$ is soil moisture (mm), and $St$ is the soil moisture capacity (mm).

$$Pe = Ft\left[\frac{S - Sl}{St - Sl}\right]^{Pow} \tag{13}$$

where $Pe$ is the percolation flow rate (mm/day), $Ft$ is the percolation at soil moisture capacity (mm/day), $Sl$ is the soil moisture storage below which no percolation occurs (mm), and $Pow$ is the power of soil moisture-percolation curve.

$$Gwft = \frac{W_G^{\frac{2}{3}}}{Gl\sqrt{St}} \tag{14}$$

where $Gwft$ is the groundwater flow rate (mm/day), $W_G$ is the groundwater storage (mm), and $Gl$ represents the groundwater delay constant (day).

Bailey and Pitman (2016) outline prescribed ranges for model variables. Internal model variables and suggested variable initial values and ranges described in Eqs. 7–14 are described in the Supplementary Information (Table S16).

#### 2.4.3 Hydrological model calibrations

In the Pitman/WRSM hydrological model, calibration statistics include the mean and standard deviation of annual runoff, log mean and standard deviation of annual runoff and the index of season flow (Bailey and Pitman 2016). These calibration statistics were deemed to be insufficient for this study. Considering the application of peak flows within FFA, metrics such as the percentage error between the simulated and observed mean annual peak flows were assessed in addition to other calibration performance statistics typically used in hydrological studies. These included the Pearson's correlation coefficient (r), the coefficient of determination ($R^2$), Kling-Gupta Efficiency (KGE) and the Nash–Sutcliffe Efficiency (NSE). Bailey and Pitman (2016) outlined a set of acceptable ranges for each variable used within the WRSM/Pitman model. Parameter adjustments were made based on these acceptable ranges after each simulation. In certain cases, adjustments were made beyond the suggested ranges. This was undertaken to evaluate the limitations of the hydrological model in projecting discharge under future climate scenarios. Further investigation was undertaken by visual inspection of simulated hydrographs.

During the calibration of the WRSM/Pitman model for selected sites, the lag of surface runoff and percolation

parameters was set to 0 days and 0.01 mm per day, respectively (Reinwarth et al. 2018). This is recommended from ephemeral rivers (Pitman 1976). In this study, the suppression of the lag variable during parameterization was implemented to maintain the peak discharge statistical profile within the simulated time series. The WRSM/Pitman model defines lag as the time delay in measuring runoff at the catchment outlet (Bailey and Pitman 2016). It was found that a higher lag parameter resulted in peak discharges being underestimated, causing a smoothing effect of daily discharge hydrographs.

This study used the Kling-Gupta Efficiency (KGE) metric as the primary calibration performance measure. The KGE statistic is advantageous in comparison to the Nash–Sutcliffe Efficiency (NSE) metric. Gupta et al. (2009) note that discharge variability is not correctly considered in the NSE. The KGE metric provides a more balanced form of the combined components of the NSE (correlation, bias, ratio of variances or coefficients of variation) (Liu 2020). In addition, the NSE metric resulted in variable performance and sensitivity in assessing maximum daily runoffs (Lin et al. 2017). As outlined in Kling et al. (2012), the KGE metric can be assessed by the following scheme:

- "Good" (KGE > 0.75),
- "Intermediate" (0.75 > KGE > 0.5),
- "Poor" (0.5 > KGE > 0),
- "Very poor" (KGE < 0).

## 2.5 Instantaneous peak flow estimation

A significant concern in FFA is the availability of precipitation data at a sub-daily time step from GCMs and hydrological models. To overcome this issue, the study adopted an empirical approach to estimate daily instantaneous peak flows (IPF) outlined in Sangal (1983) and Fuller (1914). This approach has also been taken in studies by others investigating flood frequency changes under future climate change such as Almasi and Soltani (2017). The Sangal and Fuller methods are outlined in Eqs. 15 and 16.

$$Q_{max} = \frac{\left(4Q_2 - Q_1 - Q_3\right)}{2} \tag{15}$$

where $Q_{max}$ is IPF ($m^3/s$), $Q_2$ mean daily flow at the time when peak flow occurred, $Q_1$ and $Q_3$ are daily mean flow in previous and next day of the peak ($m^3/s$).

$$Q_{max} = Q(1 + 2.66A^{-0.3}) \tag{16}$$

where $Q_{max}$ is IPF ($m^3/s$), $Q$ is mean daily flow ($m^3/s$), and $A$ is the catchment area ($km^2$).

## 2.6 Flood frequency analysis

FFA was undertaken using the AMS for IPFs at each site using the Weibull plotting position. The AMS datasets were extracted for individual GCMs and the GCM ensemble mean for the scenarios (RCP 4.5 and RCP 8.5) and future periods (2030–2060 and 2070–2100) under evaluation and the observations representing the control period (1970–2000). In addition, AMS datasets for the individual GCM and the GCM ensemble mean were extracted by the statistical downscaling and IPF estimation methods under investigation. The GCM ensemble mean represents the mean AMS series of IPF across individual GCMs for each period. Considering that the AMS is extracted from IPF data at the daily time step, the clustering of GCMs into an ensemble cannot be directly constructed by taking the mean across days within each GCM. This is due to the difference in the timing of wet and dry days across GCMs. Maimone et al. (2019) discuss this issue in further detail.

Three theoretical distributions, including the GEV, LN and LP3 distributions, were assessed for flood design estimation. These distributions were identified by Van der Spuy and du Plessis (2022) as the most commonly used distributions in South African FFA studies. Parameter estimation was undertaken using the maximum likelihood approach. The advantages of the L-moments approach, which has been applied extensively in hydrological applications, are acknowledged. Hosking and Wallis (1997) noted that the L-moments approach provided more robust parameter estimations in the presence of extreme values. Considering the application of FFA under future climate change scenarios, this study adopted the maximum likelihood method for parameter estimation owing to its application in both hydrology and climate change studies. The Kolmogorov–Smirnov, Cramér–von Mises and Chi-squared goodness of fit tests were conducted at a significance level (α) of 0.05 to determine the most suitable distribution. Test statistics are presented in Table 4. IPF quantiles were calculated for the 2-, 5-, 10-, 25-, 50-, and 100-year return periods using the selected distribution.

Chow (1954) suggested that FFA by theoretical probability distributions could be assessed using frequency factors

**Table 4** Test statistics used to assess goodness of fit

| Test | Test statistic |
|---|---|
| Chi-Squared | $\chi^2 = \sum_{i=1}^{n} \frac{(O_i - E_i)^2}{E_i}$ |
| Kolmogorov–Smirnov | $KS = max\left\lvert F(\tilde{Z}_i) - \hat{F}(\tilde{Z}_i)\right\rvert$ |
| Cramér–von Mises | $\frac{1}{12n} + \sum_{i-1}^{n}\left(\frac{2i-1}{2n} - F(\tilde{Z}_i)\right)^2$ |

'$K$' based on statistical parameters. Peak discharge ($X_T$) was calculated using Eq. 17:

$$X_T = \mu + K_T \cdot s \tag{17}$$

With the mean ($\mu$), standard deviation ($s$), and $K_T$ is the distribution-specific frequency factor for the return period $T$.

## 3 Results and discussion

### 3.1 Global circulation model ensembles and statistical downscaling outputs

Mean annual rainfall (MAR) trends are measured between the control period and climate scenarios (RCP 4.5 and RCP 8.5) under both the near (2030–2060) and long term (2070–2100). Figure 2 depicts the MAR based on the QDM downscaling method for the control period and future climate scenarios across evaluated locations in the Western Cape. The MAR estimates for the QDM, LS and DC methods are presented in Tables S1 and S3 in the Supplementary Information. A decreasing MAR trend is evident at several sites—Vredendal, Jonkershoek, Vogel Vallij and Eenzaamheid—irrespective of the downscaling method applied. For these sites, the percentage decrease in MAR between the near and long term for the RCP 4.5 scenario is less than percent decrease under RCP 8.5.

There are conflicting results between the DC, LS and QDM sites for the Stompdrift Dam and Kammanassie sites. For the DC method, there is a decreasing MAR trend detected for both sites across all scenarios and time periods, while under the QDM method, a 0.54 and 2.14% increase is present for the Kammanassie site for the near-term period (2030–2060) under RCP 4.5 and 8.5, respectively. For the Stompdrift Dam site, under the QDM method, an increase of 10.88, 11.21 and 10.78% in MAR is evident for the RCP 4.5 2030–2060, RCP 8.5 2030–2060 and RCP 4.5 2070–2100, respectively. A smaller percentage increase of 1.21% is detected under

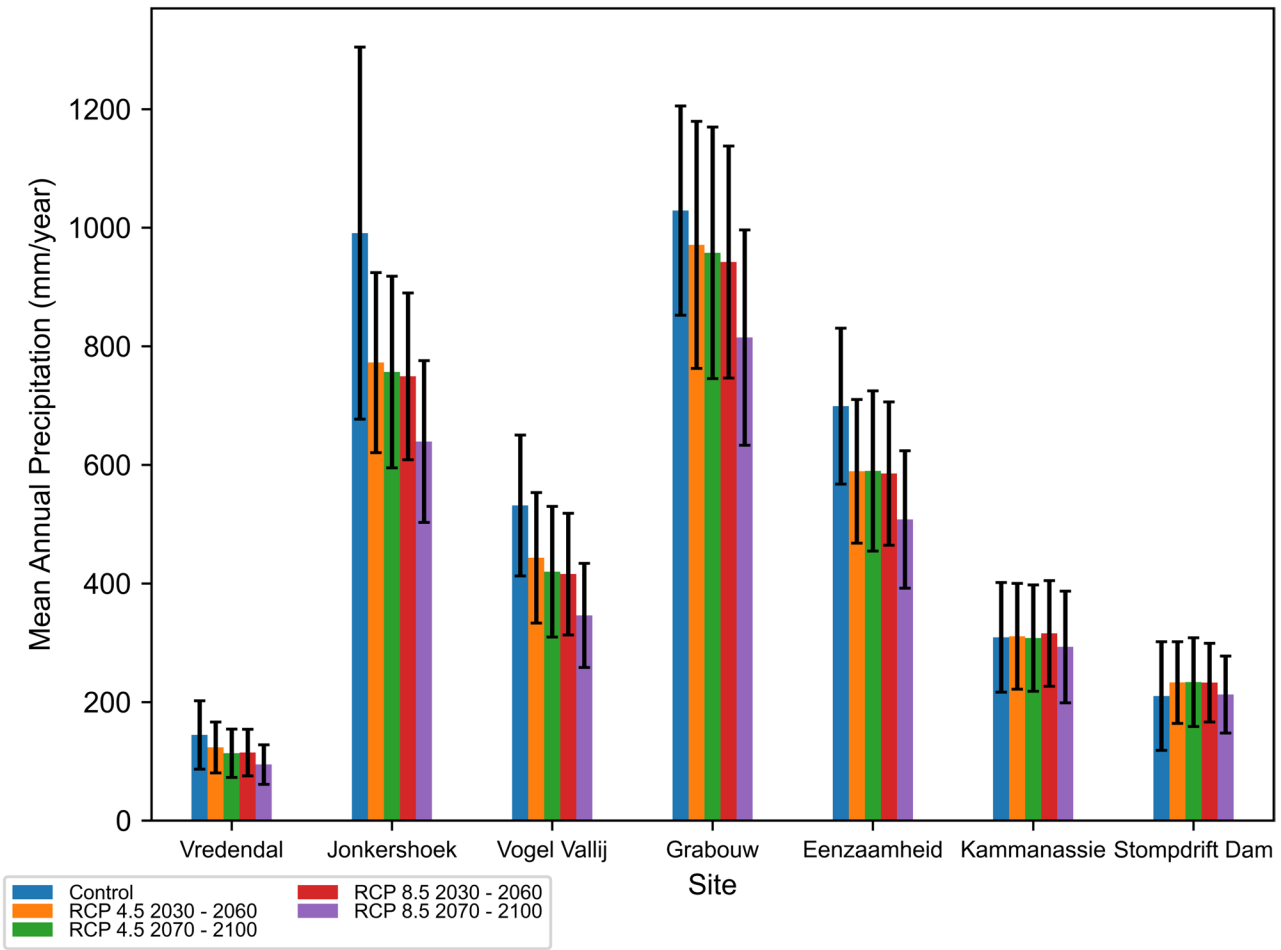


**Fig. 2** Mean annual precipitation (mm per year) with standard deviation under control and future climate scenarios across locations in the Western Cape (Downscaling Method: QDM)

the RCP 8.5 for the 2070–2100 period. For the LS downscaling method, percentage increases between 50.99 and 65.12% are detected across both scenarios and time periods for the Kammanassie site. Similarly, increases between 261.68 and 307.73% are detected for the Stompdrift Dam site. For the Grabouw site, there is consensus between the DC and QDM methods regarding the percentage decrease in MAR detected across all scenarios and periods in contrast to the percentage increases between 61.78 and 93.95% present under the LS method.

The decrease in mean annual precipitation detected across future climate scenarios for selected sites in the Western Cape concurs with the findings of several studies, including Hewitson and Crane (2006), Engelbrecht et al. (2019), Du Plessis and Kalima (2021) and Ngwenya and Simatele (2024). The decreasing rainfall trend for future climate projections follows a historical decreasing trend across the Western Cape detected by Lakhraj-Govender and Grab (2019).

Several factors may influence future changes in precipitation in the Western Cape. Decreases in the winter rainfall in the southwestern Cape and west coast have typically coincided with poleward dynamics of the southern hemisphere subtropical high-pressure belt and mid-latitude westerlies (Roffe et al. 2021; Lakhraj-Govender and Grab 2019). Poleward shifts of moisture corridors can be attributed to the Southern Annular Mode and the expansion of the sub-tropical anticyclones in the South Atlantic and South Indian Ocean (Lakhraj-Govender and Grab 2019). Changes in Antarctic sea ice and the expansion of the Hadley cell are likely to result in changes in rainfall for regions that derive moisture from the mid-latitudes (Pascale et al. 2016; Roffe et al. 2021). Changes in climate modes such as the Southern Oscillation Index and solar (sunspot) activity may also contribute to inter-annual rainfall variability in the Western Cape (Ndebele et al. 2020, 2022; Mazibuko et al. 2021).

### 3.2 Hydrological modelling

Average daily discharge simulations were run on seven pairs of precipitation stations and river gauges across the Western Cape. Calibration and parameterization of the WRSM/Pitman daily model were undertaken by comparing observed and simulated average daily discharge generated from observed daily precipitation for the control period (1970–2000). Results from the calibration are presented in Table 5 and calibration hydrographs in Fig. 3. Of the seven pairs calibrated, no calibrations within the "good" category were achieved for the KGE metric. Calibrations with "intermediate" results for the KGE metric were achieved for the Jonkershoek, Little Berg River, and Palmiet sites. The assessment of percentage error between observed and simulated mean annual peak flows resulted in acceptable thresholds (percentage error < 10%) for the Doring River, Jonkershoek, Little Berg River, Palmiet and Marnewicks River according to guidelines outlined in Bailey and Pitman (2016). Considering the findings across calibration performance statistics, only the Jonkershoek and Little Berg River were assessed further within the FFA.

The influence of the selected hydrological model on climate change FFA has been noted in several studies, such as Maurer et al. (2018), Mizukami et al. (2016) and Mendoza et al. (2015). These studies suggest that the choice of hydrological model and rigour of the calibration is a more significant contributor to uncertainty than other methodological choices. This is also a significant finding in this study. The successful calibration of hydrological models is complex in Southern Africa since less than 9% of mean annual precipitation is converted into mean annual runoff, while 5% recharges groundwater (Fikileni and Wolski 2022; Edokpayi et al. 2020). Despite this regional trend, an investigation by Lakhraj-Govender and Grab (2019) detected significant correlations between annual rainfall and annual river flows at several sites across the Western Cape.

The WRSM/Pitman model had limited success in simulating flows at river gauges in the Western Cape. Of the

**Table 5** Calibration performance statistics across locations in the Western Cape

| Site | Simulated Mean Annual Peak Flows ($m^3/s$) | Observed Mean Peak Flows ($m^3/s$) | Percentage Error (%) | Kling-Gupta Efficiency (KGE) | Pearsons Correlation Coefficient (r) | Coefficient of Determination ($R^2$) |
|---|---|---|---|---|---|---|
| Doring River | 297.02 | 303.09 | − 2.00 | 0.401 | 0.403 | 16.25 |
| Jonkershoek | 11.36 | 10.97 | 3.60 | 0.650 | 0.674 | 45.43 |
| Little Berg River | 51.22 | 51.76 | − 1.03 | 0.579 | 0.601 | 36.08 |
| Palmiet | 42.59 | 40.63 | 4.83 | 0.539 | 0.545 | 29.72 |
| Hermitage | 7.40 | 8.58 | − 13.81 | 0.383 | 0.412 | 16.96 |
| Marnewicks River | 0.192 | 0.185 | 3.48 | 0.401 | 0.412 | 16.96 |
| Vermaaks River | 0.35 | 0.41 | − 13.55 | 0.078 | 0.259 | 6.69 |

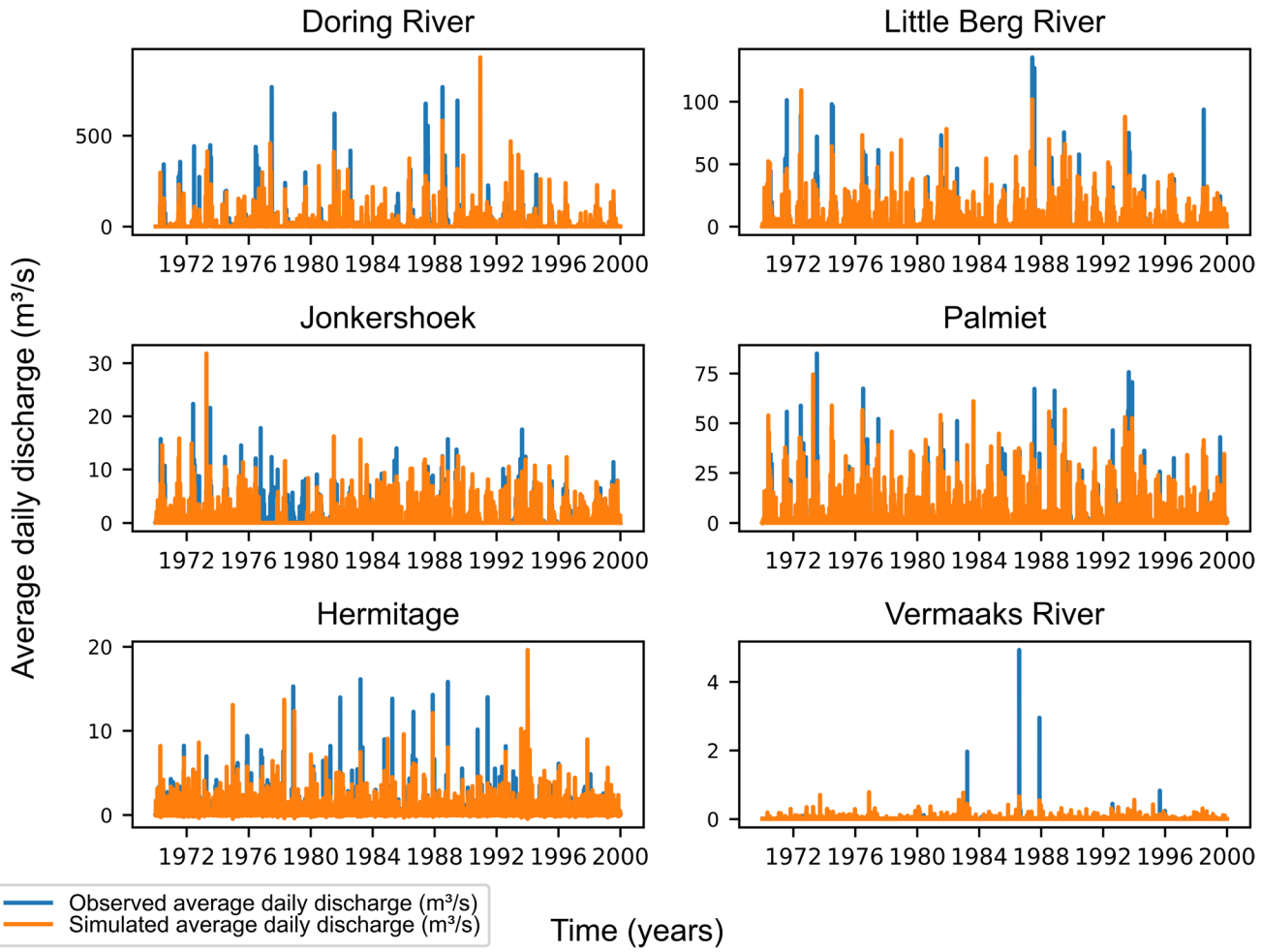


**Fig. 3** Hydrographs of observed and simulated daily discharge ($m^3/s$) for selected sites

seven sites investigated, two sites obtained acceptable calibrations; however, the strength of KGE scores for these sites were only in the "intermediate" category described by Kling et al. (2012). Several factors could be attributed to the calibration performance of the WRSM/Pitman model. First, the model was developed using rainfall stations in Pretoria in the Gauteng province of South Africa. In addition, there is a spatial and seasonal variation in rainfall in South Africa. The Gauteng province receives most of its rainfall in summer in the form of orographic or convective showers. At the same time, the Western Cape experiences winter rainfall that originates from cyclones over the South Atlantic (du Plessis and Schloms 2017; Roffe et al. 2019). Therefore, the derivation of storm event duration and rainfall amounts within the WRSM/Pitman model may be more suitable for areas with convective rainfall (locally limited), with a prevalence of cumulonimbus-induced thundershowers and frontal rainfall.

The semi-arid climate may have also influenced calibrations of the WRSM/Pitman model in the Western Cape. Andersson et al. (2011) also noted challenges using hydrological models in arid climates in Southern Africa. Flood design estimation is challenging in arid and semi-arid areas owing to the high variability in rainfall, inter-annual vegetation cover and intermittent streamflows (Zaman et al. 2012). Flow measurement may also be problematic in semi-arid areas due to siltation of inlet pipes at river gauges (Zaman et al. 2012). Cordery and Fraser (2000) stated that flooding events that occurred in arid regions were usually a result of high-intensity storms over a smaller area of the catchment. Therefore, flooding variability is much greater across arid regions than in other areas (Zaman et al. 2012; Cordery and Fraser 2000; Farquharson et al. 1992).

Poor hydrological model calibrations may also be attributed to catchment size variability. Smaller catchments are more challenging to model as the drivers of hydrological flow, beyond surface runoff and groundwater processes, may be significant. Watson et al. (2021) noted that for small catchments in the Western Cape, such as the Verlorenvlei and Bot, evapotranspiration, simulating days of zero flow and baseflow could dampen the hydrological response of

catchments. Furthermore, the use of lumped hydrological models, such as the WRSM/Pitman model, can be problematic as they cannot simulate certain model elements, such as slow declines in groundwater storage (Watson et al. 2021).

### 3.3 Instantaneous peak flows

Figure 4 depicts changes in the mean daily IPF ($m^3/s$) under the control and future climate scenarios and time periods based on the Fuller and Sangal IPF estimation methods. IPF estimates using the Fuller method are higher under all scenarios for both sites compared to estimates based on the Sangal method. There is agreement between both methods on the decrease in mean daily IPFs detected across all scenarios for both sites. The percentage decrease in mean daily IPF is largest under the RCP 8.5 2070–2100 scenario at both sites. The higher percent decreases in IPF are present for the Little Berg River site. Under the Fuller method, there is between a 38.95 and 85.76% decrease in mean daily IPF across all scenarios. Additionally, in the case of the Jonkershoek site, percentage decreases in mean daily IPF are lower in comparison to the Little Berg River. Under the RCP 4.5 2030–2060, RCP 4.5 2070–2100 and RCP 8.5 2030–2060 scenarios, mean daily IPF decreased by − 27.94, − 30.64, and − 31.91%, respectively (Fuller method). Tables 6 and 7 summarize the percentage changes in estimated mean daily IPF for the control and future climate scenarios across selected sites using the Fuller and Sangal methods, respectively.

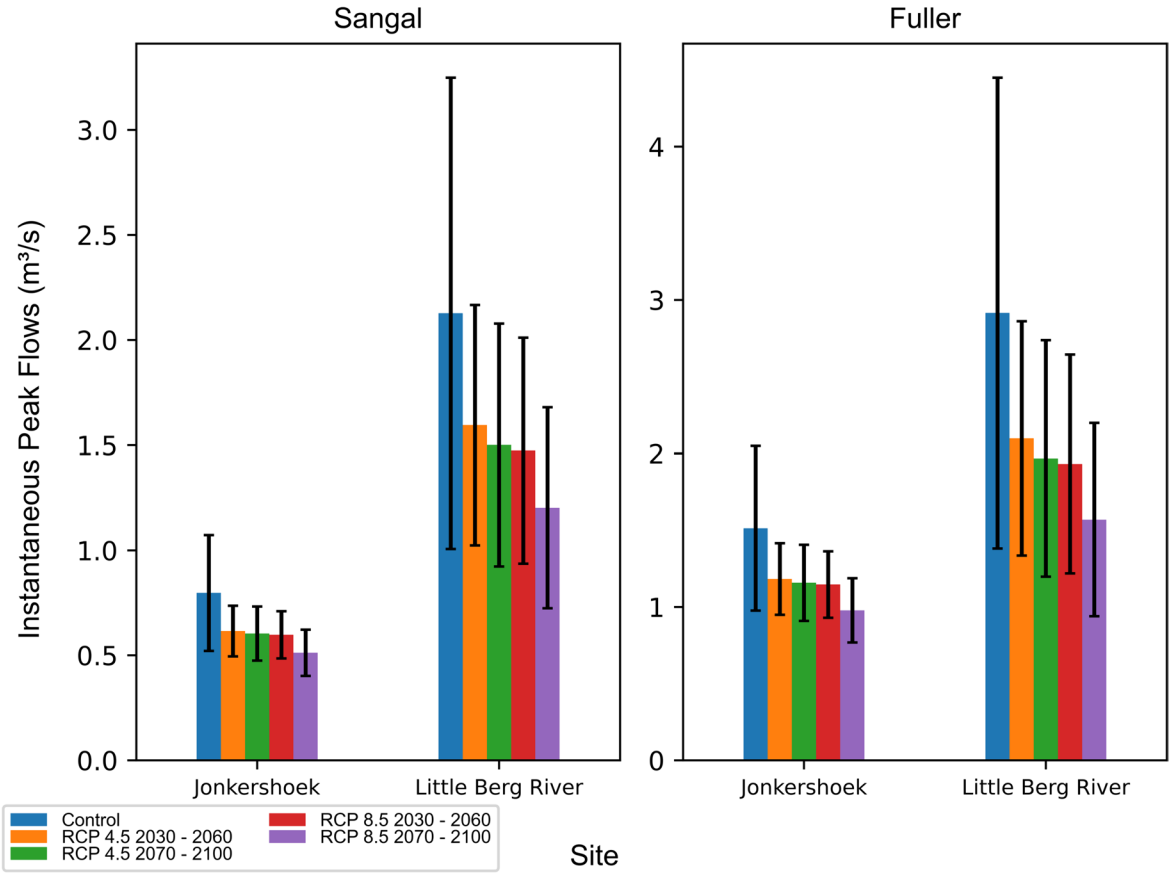


**Fig. 4** Estimated mean daily IPF ($m^3/s$) with standard deviation under control and future climate scenarios for the Sangal and Fuller methods (GCM Ensemble; Downscaling Method: QDM)

**Table 6** Percentage change in Fuller estimated IPFs ($m^3/s$) between control and future climate scenarios across selected sites in the Western Cape (GCM Ensemble; Downscaling Method: QDM)

| Site | Control ($m^3/s$) | RCP 4.5 2030–2060 | RCP 4.5 2070–2100 | RCP 8.5 2030–2060 | RCP 8.5 2070–2100 |
|---|---|---|---|---|---|
| Jonkershoek | 1.513 | − 27.94% | − 30.64% | − 31.91% | − 54.66% |
| Little Berg River | 2.915 | − 38.95% | − 48.14% | − 50.89% | − 85.76% |

**Table 7** Percentage change in Sangal estimated IPFs ($m^3/s$) between control and future climate scenarios across selected sites in the Western Cape (GCM Ensemble; Downscaling Method: QDM)

| Site | Control ($m^3/s$) | RCP 4.5 2040–2060 | RCP 4.5 2080–2100 | RCP 8.5 2040–2060 | RCP 8.5 2080–2100 |
|---|---|---|---|---|---|
| Jonkershoek | 0.797 | − 29.41% | − 31.96% | − 33.28% | − 55.58% |
| Little Berg River | 2.127 | − 33.37% | − 41.78% | − 44.37% | − 76.98% |

The finding of reduced mean daily IPFs under future climate change concurs with other studies undertaken in the region. Edokpayi et al. (2020) reported a projected reduction of 20–60% in annual runoff under an unconstrained mitigation scenario, while a 5–20% decrease could be realized under a constrained scenario. A study of the Eerste River in the Western Cape also found a projected reduction in river flows of between 8 and 18% (Du Plessis and Kalima 2021), while Cullis et al. (2015) noted that flow reductions were notable in the southwestern Cape catchments under all climate models assessed. Decreases in mean daily IPF follow the decreases in historical river flow across the Western Cape identified by Lakhraj-Govender and Grab (2019).

Studies evaluating the impact of climate change on hydrological flow have found that projected rainfall plays a significant role in flow variability (Arnell and Gosling 2013). This is also true in South Africa (Edokpayi et al. 2020). A study by Davis et al. (2010) found that an 8% reduction in annual rainfall could result in a 30 and 31% decrease in surface runoff and groundwater, respectively. In addition, reduced IPFs under future climate change can be attributed to the potential increase in evaporation rates and temperature and changes to the timing of rainfall. Arnell (1999) predicted a reduction in river flow of between 26 and 40% of the Zambezi River system and a 40% increase in evaporation. Reduced river flow cannot be solely attributed to climate change. Lakhraj-Govender and Grab (2019) stated that historical variations in river flow indicated that both anthropogenic (water abstraction for agriculture and land use change) and natural (increased evaporation, ENSO phases, catchment size) factors were influential.

## 3.4 Flood frequency analysis

### 3.4.1 Distribution fitting and selection

Based on the Kolmogorov–Smirnov, Cramér–von Mises and Chi-squared goodness of fit tests with a confidence level of 95% ($\alpha > 0.05$), the LP3 distribution was selected as the most suitable distribution based on its consistency across all sites, scenarios and IPF and downscaling methods. For several scenarios under the DC method, the LN performed poorly in terms of its statistical significance under goodness of fit tests. A sample of the Kolmogorov–Smirnov goodness of fit tests are provided in supplementary material (Tables S4 to S15 in the Supplementary Information). Generally, the results demonstrate that the flood frequency distribution does not change under future scenarios. Figure 5 provides an overview of fitted distributions under control and future scenarios for the Little Berg River using the QDM downscaling and Fuller IPF methods. Figures S1–S3 in the Supplementary Information depict distribution fitting for the Little Berg River using the IPF Sangal Method and both methods for the Jonkershoek.

### 3.4.2 FFA by downscaling method

Figures 6 and 7 illustrate the change in FFCs under different statistical downscaling methods for the Jonkershoek and Little Berg River based on the Fuller and Sangal IPF methods. There is agreement between the LS and QDM downscaling methods for both sites where FFCs exhibit a decreasing trend across all future climate scenarios in comparison to the control scenario. Under the DC method, FFCs show a decreasing trend for high-probability events (1 in 2, 1 in 5, 1 in 10). At the same time, the FFC curves are higher than the control scenario for high-severity events (> 1 in 10). There is agreement in FFCs trends between the Fuller and Sangal IPF methods between both sites for the LS and QDM methods. Under the DC method, there is a difference detected between the Fuller and Sangal methods for the Little Berg River where the Sangal FFCs under future scenarios show a decreasing trend in comparison to the control scenario except for the RCP 4.5 2070–2100.

As noted in Figs. 6 and 7, the DC method performed inconsistently across the Jonkershoek and Little Berg River sites compared to the LS and QDM methods. The DC method assumes stationarity as the relative correction factor is applied to the control period observed rainfall. The method maintains wet days and reduces the daily climate variability associated with raw GCM outputs (Tabari et al. 2021). However, Shaw and Riha (2011) noted that the use of DC downscaling resulted in an underestimation in the range of uncertainties from the GCM or RCM outputs as it was based on changes in mean climate across periods.

In this study, there was agreement between the LS and QDM methods regarding the direction of FFCs; however, quantiles generated using the LS approach were generally lower compared to the QDM approach. This suggests that peak flows may be underestimated under the LS approach.

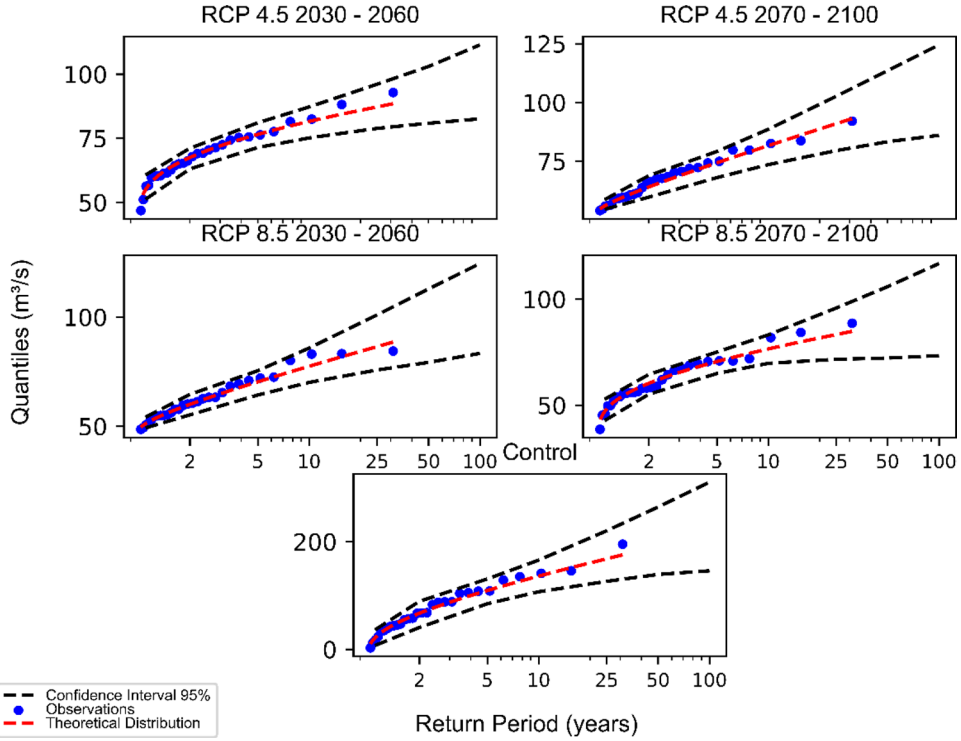


**Fig. 5** Fitting LP3 distributions to IPFs for the control and future scenarios for Little Berg River (GCM ensemble mean; Downscaling Method: QDM; IPF Estimation Method: Fuller)

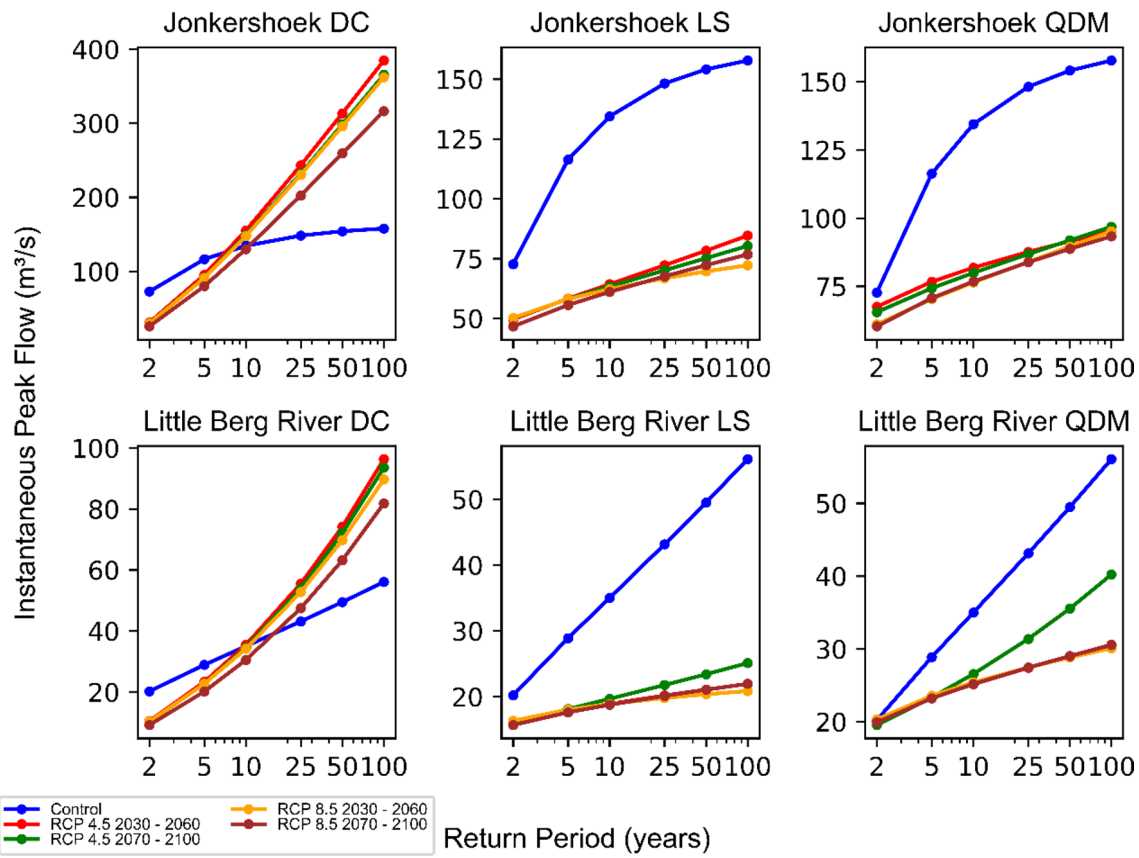


**Fig. 6** LP3 FFCs fitted under control and future scenarios for Jonkershoek and Little Berg River (GCM ensemble mean; Downscaling Method: DC, LS and QDM; IPF Estimation Method: Fuller)

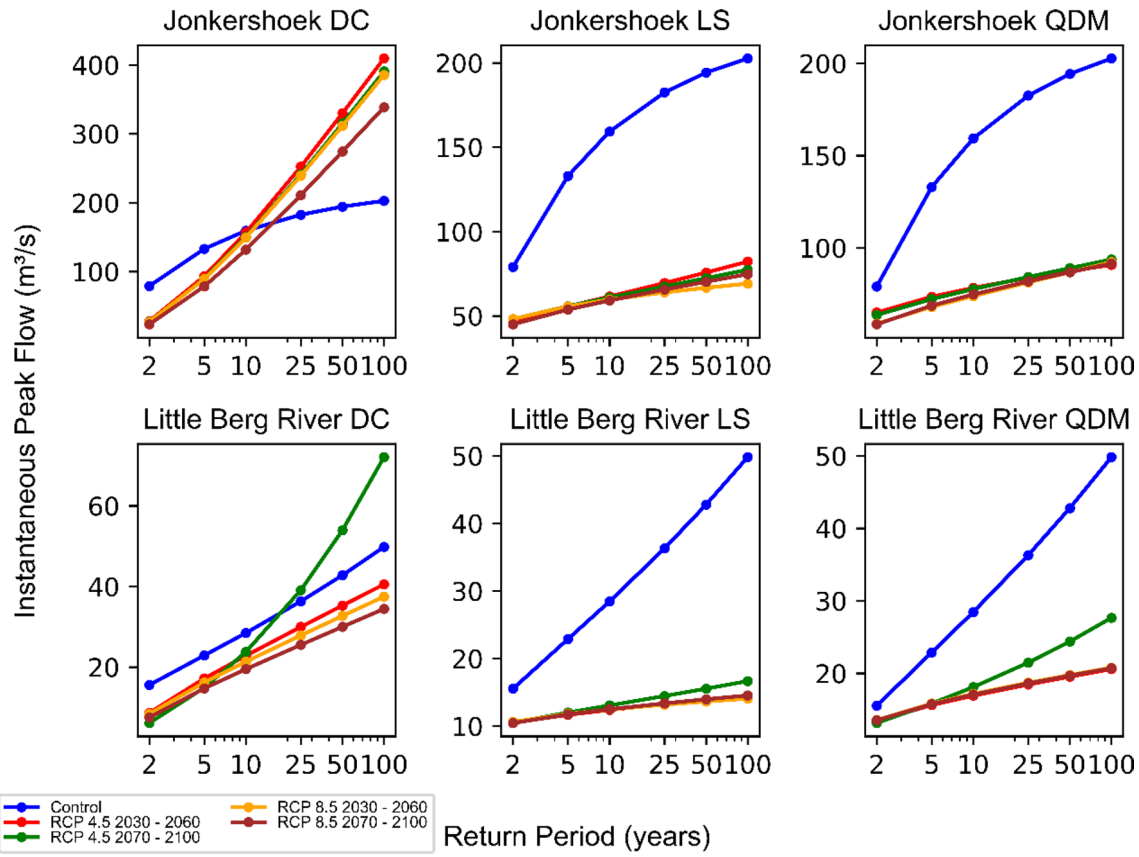


**Fig. 7** LP3 FFCs fitted under control and future scenarios for Jonkershoek and Little Berg River (GCM ensemble mean; Downscaling Method: DC, LS and QDM; IPF Estimation Method: Sangal)

Soriano et al. (2019) and Dobler et al. (2012). Soriano et al. (2019) note that only advanced statistical downscaling methods, such as the QDM approach, were suitable for reproducing peak flows. Quantile mapping methods are also recommended for temperature projections (Fan et al. 2021). More broadly, Chen et al. (2011) state that the choice of the downscaling method is the largest source of uncertainty with respect to specific elements that might influence FFA, such as spring mean discharge, annual low flow, and peak discharge.

### 3.4.3 FFA by climate model

Figures 8 and 9 depict FFCs for different climate models at the Little Berg River and Jonkershoek sites under the QDM downscaling and Fuller IPF methods. For the Little Berg River site, FFCs representing individual downscaled GCMs generally exhibit a decreasing trend for future scenarios compared to the control scenario for high-probability events. In contrast, selected individual GCMs result in an increasing flood frequency trend. For example, under the RCP 4.5 2030–2060 scenario, the CanESM2, MRI-CGCM3 and ACCESS1-0 are higher than the control scenario for return periods greater than 1 in 25.

The FFCs for individual GCMs for Jonkershoek lie closer to the control scenario FFC for the RCP 4.5 2030–2060, RCP 4.5 2070–2100 and RCP 8.5 2030–2060, suggesting that there is less variability between GCMs and greater model agreement regarding the decreasing trend in FFCs under future climate scenarios. Under all future scenarios for both sites, FFCs estimated using the GCM ensemble mean are below the control scenario in addition to a majority of individual GCMs.

GCMs may vary in their ability to reproduce rainfall distribution statistics, seasonality patterns, and extremes (Hughes et al. 2014). According to Arnell et al. (Arnell et al. 2003), GCMs that overestimate rainfall also tend to overestimate runoff. Therefore, the choice of GCM is crucial in determining the direction of the FFCs across the Jonkershoek and Little Berg River sites. This finding aligns with Camici et al. (2014) and Kay et al. (2009). Furthermore, FFCs based on IPFs may introduce further complexity if GCMs cannot capture extreme rainfall statistics. Andersson et al. (2011) found decreased river flow; however, there was

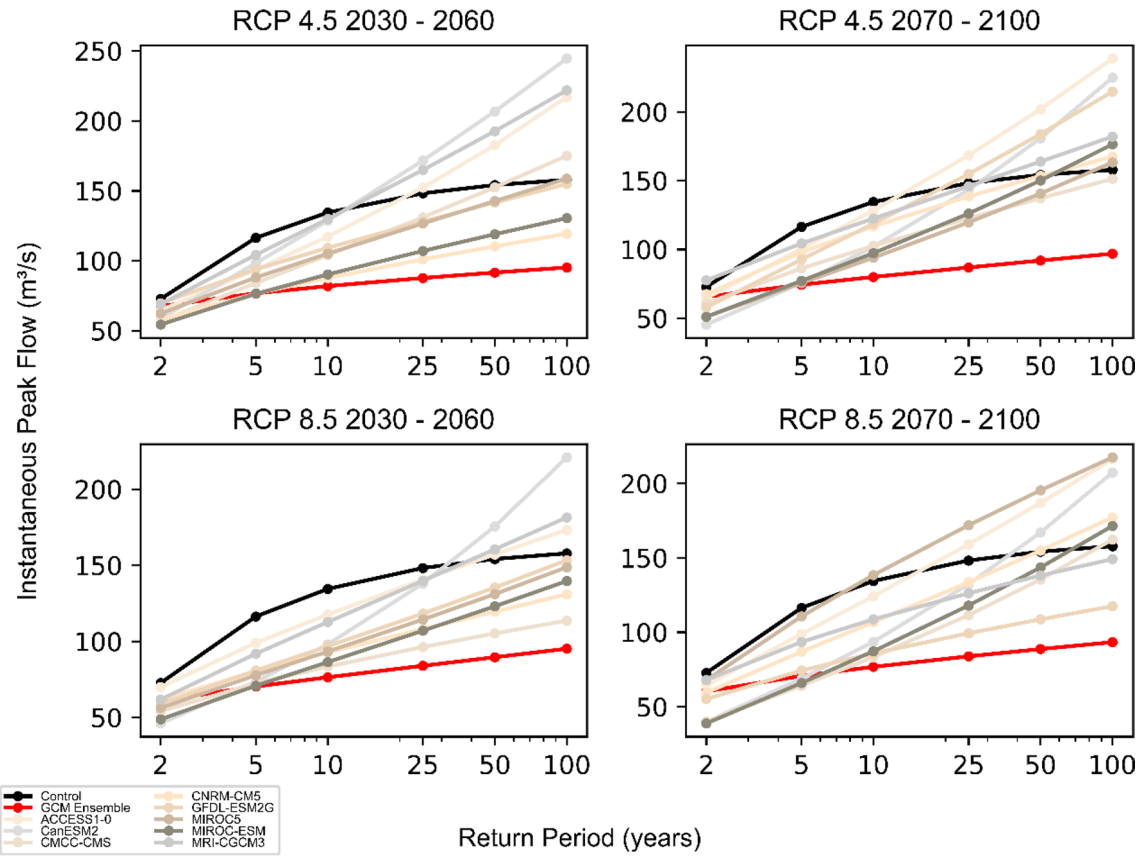


**Fig. 8** LP3 fitted FFCs by climate model for future scenarios at Little Berg River (Downscaling Method: QDM; IPF Estimation Method: Fuller)

no consensus between climate models on increased risks of high flows.

GCMs inherently possess systematic errors because of conceptual deficiencies (Stergiou et al. 2021). In addition, the simulation of extreme precipitation continues to be an issue within GCMs owing to variations in model considerations of diurnal cycles in convective rainfall and its integration at coarse resolutions (Bulti et al. 2021; Chokkavarapu and Mandla 2019; Dedekind et al. 2016). This is also the case in the Western Cape, where despite the broad consensus regarding the projected decreases in winter rainfall, there are large areas of disagreement between models. Hewitson and Crane (2006) also suggest that this may be owing to the varied precipitation parameterization within GCMs and the integration of local conditions and feedback mechanisms (Andersson et al. 2011).

GCMs may be able to simulate extreme rainfall over the west coast regions (Mason and Joubert 1997). However, GCMs tend to overestimate rainfall over the southwest coast of South Africa (Mason and Joubert 1997). Studies evaluating GCM skill in South African catchments conclude that GCM models such as those developed by Goddard Institute for Space Studies and Max Planck Institute are more skilled than others (Hughes et al. 2014). However, these models may still vary in their consistency across coastal and inland regions. Hughes et al. (2014) noted that only a limited reduction in the overall uncertainty is attained when using skilled GCM outputs in a hydrological modelling context.

Changes in rainfall can alter the distribution of water spatially and temporally within a catchment area (Edokpayi et al. 2020). The use of coarse or low-resolution GCMs (300 km × 300 km) can be problematic as there is a scale mismatch with hydrological models, which typically operate at the catchment scale (± 50 km × 50 km) (Mareuil et al. 2007; Chokkavarapu and Mandla 2019; Watson et al. 2021). Hydrological flows depend on feedback loops and dependencies within different processes and land features (Watson et al. 2021). Finer resolution climate models would be able to capture variables at the local scale more accurately, thereby ensuring that investigations of hydrological catchments are more robust (Andersson et al. 2011). In the Western Cape, there is a strong correlation between elevation and rainfall; for example, high flows in the Breede and Berg catchments are derived from surface run-off from increased precipitation in mountainous areas (Watson et al. 2021). Simulating precipitation over pronounced topography is a notable challenge for GCMs (Andersson et al. 2011). Therefore, extreme flows and, consequently, FFCs may be

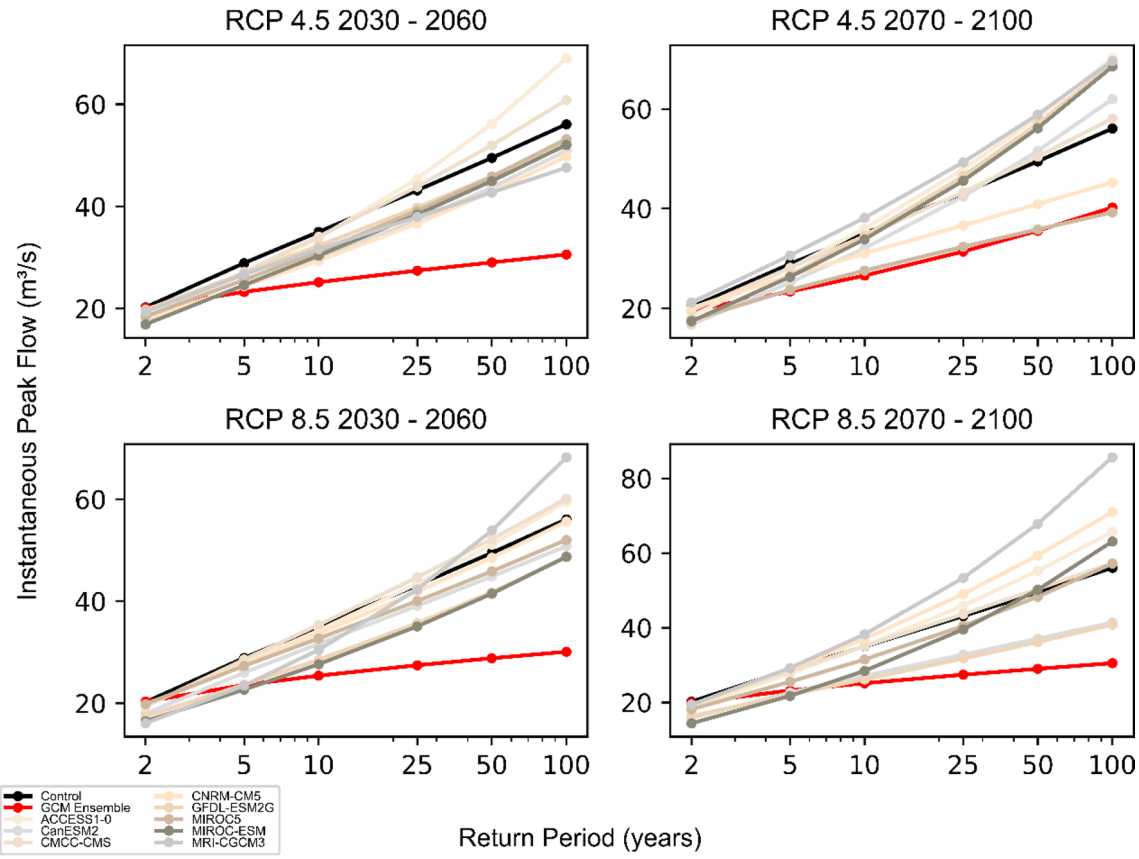


**Fig. 9** LP3 fitted FFCs by climate model for future scenarios at Jonkershoek (Downscaling Method: QDM; IPF Estimation Method: Fuller)

underestimated in the Western Cape. Furthermore, if GCMs do not correctly capture spatial patterns of rainfall, extreme flows may be incorrectly located.

RCMs could address the scale issue if they are able to appropriately capture regional and local climate (Arnell and Jones 2003). Using RCMs is only advantageous if the driving GCM can capture regional variability in projected climate variables. As Andersson et al. (2011) mentioned, the forcing GCM is still responsible for transmitting the broad signal. The reliability of RCM projections is relatively unknown in the Western Cape (Abiodun et al. 2016). All Coordinated Regional Downscaling Experiment RCMs under-estimate extreme rainfall threshold values in the Western Cape (Abiodun et al. 2016).

To overcome the variability in extreme precipitation outputs from GCMs, a GCM ensemble is recommended (Fan et al. 2021; Camici et al. 2014; Qin and Lu 2014). The structure of the GCM ensemble is critical. In this study, FFCs related to the GCM ensemble mean mostly exhibited a decreasing trend in comparison to individual GCM FFCs and the FFC of the control period (Figs. 8 and 9). This finding is highlighted by Giuntoli et al. (2021). The multi-model GCM ensemble based on the mean across GCMs can suppress AMS for distribution fitting. This can complicate the assessment of the direction of FFCs under future climate scenarios. Other studies have attempted to overcome this issue by using the median across the GCM ensemble (Qin and Lu 2014) or more advanced methods such as Bayesian hierarchical models (Giuntoli et al. 2021).

#### 3.4.4 FFA by IPF method

Figure 10 depicts the fitted FFCs for the GCM ensemble mean under the Fuller and Sangal IPF estimation methods. For both IPF estimation methods, a decreasing trend is evident in all scenarios across both sites compared to the control scenario. At the Little Berg River location, IPF for the 1 in 2 flood magnitude decreased by between 7.68 and 20.55% under the Fuller method. The highest percentage decreases have occurred within the RCP 8.5 2070–2100 scenario for all return periods. The percentage decreases for the 1 in 100 flood magnitudes range between 65.84 and 69.08%. The Jonkershoek site exhibits a similar trend to the Little Berg River site. Under high probability events such as the 1 in 2 return period, percentage differences between estimated quantiles are small across all scenarios, ranging from a 0.53% increase to a 3.44% decrease. In comparison, a range of percentage decreases between 39.22–83.67% is evident

for the 1 in 100 return period. Quantile estimates for Little Berg River and the Jonkershoek for the 2-, 5-, 10-, 25-, 50-, and 100-year return periods under control and future climate scenarios are provided in Tables 8 and 9, respectively.

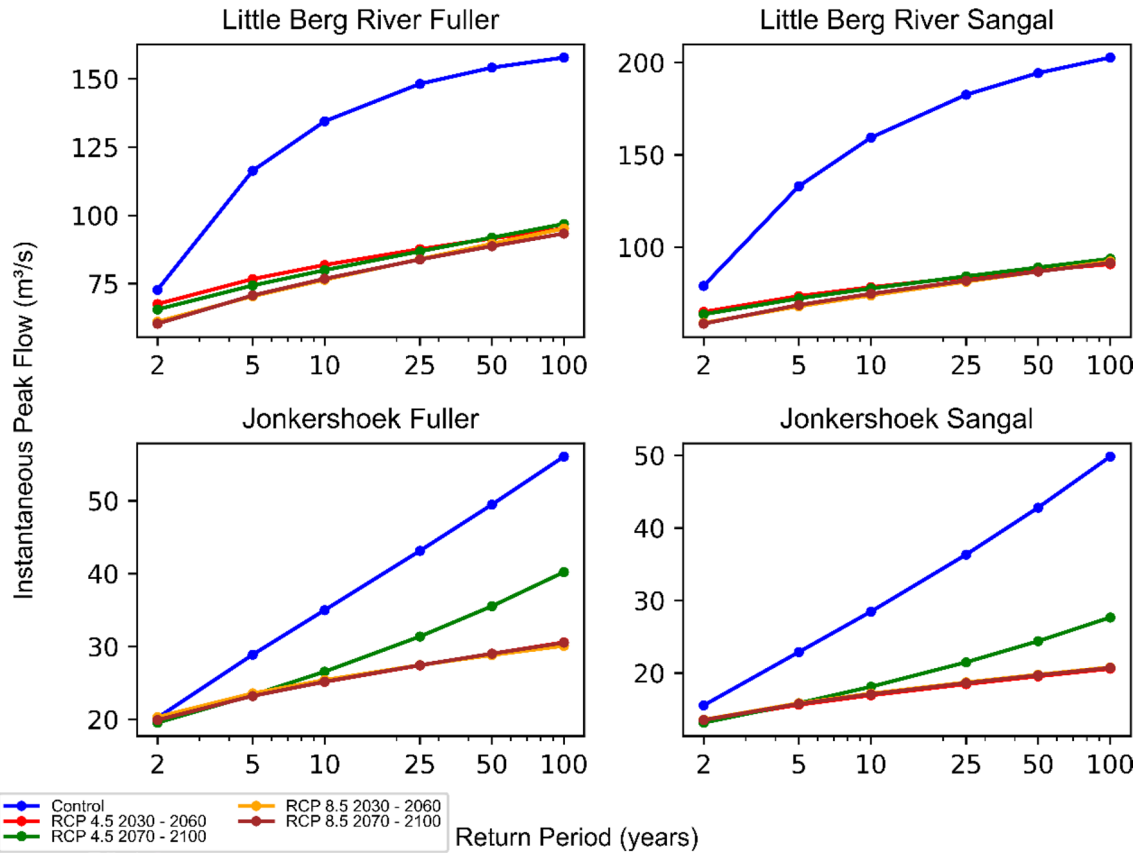


**Fig. 10** LP3 fitted FFCs under control and future scenarios for Jonkershoek and Little Berg River (GCM ensemble mean; Downscaling Method: QDM; IPF Estimation Method: Fuller and Sangal)

**Table 8** Design flood estimates for the Little Berg River under control and future climate scenarios (GCM Ensemble; Downscaling Method: QDM; IPF Estimation Method: Fuller)

| Scenario | Return Period (year) | | | | | |
|---|---|---|---|---|---|---|
| | 2 | 5 | 10 | 25 | 50 | 100 |
| Control | 72.69 | 116.34 | 134.45 | 148.18 | 154.12 | 157.82 |
| RCP 4.5 2030–2060 | − 7.68% | − 51.73% | − 64.29% | − 69.10% | − 68.37% | − 65.84% |
| RCP 4.5 2070–2100 | − 10.93% | − 56.55% | − 68.24% | − 70.68% | − 67.77% | − 62.95% |
| RCP 8.5 2030–2060 | − 19.07% | − 65.37% | − 75.99% | − 76.48% | − 72.06% | − 65.82% |
| RCP 8.5 2070–2100 | − 20.55% | − 64.62% | − 75.15% | − 76.79% | − 73.74% | − 69.08% |

**Table 9** Design flood estimates for the Jonkershoek under control and future climate scenarios (GCM Ensemble; Downscaling Method: QDM; IPF Estimation Method: Fuller)

| Scenario | Return Period (year) | | | | | |
|---|---|---|---|---|---|---|
| | 2 | 5 | 10 | 25 | 50 | 100 |
| Control | 20.22 | 28.89 | 35.00 | 43.13 | 49.48 | 56.07 |
| RCP 4.5 2030–2060 | − 0.39% | − 24.22% | − 39.16% | − 57.34% | − 70.49% | − 83.37% |
| RCP 4.5 2070–2100 | − 3.44% | − 23.74% | − 31.82% | − 37.48% | − 39.22% | − 39.40% |
| RCP 8.5 2030–2060 | 0.53% | − 22.51% | − 37.76% | − 57.12% | − 71.64% | − 86.29% |
| RCP 8.5 2070–2100 | − 1.50% | − 24.41% | − 39.06% | − 57.18% | − 70.48% | − 83.67% |

A comparison of the IPF estimation method is not possible within this research as observed data is unavailable at the sub-daily timestep. Differences between the Fuller and Sangal methods in determining the direction of FFCs are discussed in Almasi and Soltani (2017). This study notes that the Fuller IPF estimation method may be less efficient in the Western Cape as it only integrates catchment area into its formulation, excluding other variables such as slope, land use and land cover, soil drainage and moisture. Hydrological flow in the Western Cape is driven by surface runoff from mountainous regions and regional ground flow (Watson et al. 2021). Therefore, slope-related variables should be integrated into IPF estimation approaches.

Lee et al. (2020) undertook a comparison of empirical IPF methods. The study found that the Fuller method had the worst performance, leading to a significant underestimation of peak flows. However, others, such as Maghsood et al. (2019) and Jimeno-Sáez et al. (2017), successfully estimated IPFs using the approach. Several studies have adjusted the Fuller equation for use in different regions (Jimeno-Sáez et al. 2017). The Sangal method may also be inefficient and has been found to underestimate (Loyeh and Bavani 2021) and overestimate peak flows (Chen et al. 2017). The issue is acute in studies focused on small catchments or large flow events. The Sangal method was developed on a peak flow dataset during snowmelt (Chen et al. 2017). Therefore, its performance in the Western Cape may not be appropriate as extreme rainfall events typically drive high flows.

## 4 Conclusions and recommendations

This study found that FFCs using a GCM ensemble based on mean AMS exhibited a decreasing trend at the Little Berg River and Jonkershoek sites. These results were found for the LS and QDM downscaling methods (irrespective of the IPF method). In contrast, an increasing trend was found for low probability return periods under the DC method. The QDM is deemed a suitable downscaling method for projecting extreme peak flows. Despite the consensus in the decreasing trend in FFCs for the Sangal and Fuller methods using QDM downscaling, individual GCMs were found to significantly influence the direction of FFCs. Therefore, the selection of GCMs in an ensemble is critical. The assessment of suitable GCMs for climate change FFA cannot simply rely on their projection skill; they must also consider their applicability to the regional context, their ability to integrate local scale features and their precipitation parameterization approaches. It is important to note that although empirical downscaling can allow for projections that are consistent with circulation patterns, it is not capable of integrating local-scale feedback (Hewitson and Crane 2006). Other downscaling methods could be used to enhance the FFA in South Africa. Hewitson and Crane (2006) showed that the self-organizing maps downscaling approach has been successful in capturing the spatial pattern of rainfall across the Western Cape. There is consensus between IPF methods; however, quantile estimations are lower under the Fuller method in comparison to the Sangal method for high-magnitude events.

Hydrological homogeneity in the future cannot be assumed owing to climate change drivers. Therefore, incorporating climate change aspects into FFA must be carefully considered. Climate change FFA is limited because methodologies, approaches and techniques emanate from two separate disciplines: hydrology and climate science. Variations in the direction of the FFCs are caused by uncertainty from methodological choices with respect to GCMs, downscaling approaches and hydrological models and their calibration (Xu et al. 2005). Further research is required if quantile estimations can be used for practical applications. Future studies on climate change FFA in South Africa should incorporate other advanced statistical and dynamical downscaling methods, alternative approaches to extract the GCM ensemble peak flows and GCM skill evaluations for precipitation. This study concludes with the following recommendations that aim to provide methodological insights based on this research for future studies conducted in the region.

### 4.1 Recommendations

*Overcoming data availability challenges:* Smithers (2012) notes the need for design flood estimation in smaller South African catchments. However, most of these catchments remain ungauged; therefore, observed discharge data is unavailable for these locations. Since the 1970s, there has been a notable decline in the number of operational rainfall stations providing reliable hydrological information; this is problematic (Pitman and Bailey 2021). Future studies could incorporate the use of satellite quasi-precipitation products such as the Climate Hazards Group InfraRed Precipitation with Station data (CHIRPS), which can overcome reliability and completeness issues of observed rainfall datasets in South Africa (Pitman and Bailey 2021).

*GCM Uncertainty:* It is widely acknowledged that the uncertainty within GCMs can play a crucial role in influencing the reliability of hydrological studies incorporating climate change considerations (Hawkins and Sutton 2011; Najafi et al. 2011). Future studies must continue to assess GCM performance within climate change FFA studies (Bannister et al. 2017; Miao et al. 2014) while incorporating the use of multi-model GCM ensembles can enhance the reliability of future climate projections (Jose et al. 2022). RCMs may be better suited to hydrological studies that cover a catchment scale or areas with complex topography (Kim et al. 2021).

*Downscaling methods:* Future climate change FFA studies should focus on the use of more advanced statistical downscaling methods such as quantile mapping and stochastic weather generators to better assess flood frequency trends in the Western Cape. Quantile mapping methods are advantageous as they are able to simulate peak flows in comparison to the DC and LS method. Khazaei et al. (2012) proved the feasibility of using a weather generator to simulate rainfall and temperature data as inputs of a rainfall-runoff model for climate change impact assessment on floods in Iran. In addition, the study highlighted that weather generators could produce long-time series, which can overcome the issue of short record lengths in FFA.

*Hydrological Modelling:* Hydrological models that exhibit the storm duration and rainfall trends of the study area must be selected. In this study, the WRSM/Pitman model limited the analysis as successful calibrations were not possible at all sites. Often, hydrological models are "black boxes" that do not disclose their mathematical framework. This results in difficulty in determining whether the hydrological model is suitable or how the modelling framework can be adapted to be locally appropriate. In terms of applying the WRSM/Pitman model in the Western Cape, mathematical equations describing the relationship between the storm event duration and rainfall would need to be redeveloped using historical data from weather stations based in the province.

**Supplementary Information** The online version contains supplementary material available at https://doi.org/10.1007/s00477-024-02786-0.

**Author Contribution** KP was responsible for the original draft preparation, conceptualization, methodology, data curation, coding and analysis, and writing—review and editing while DMS was responsible for supervision, review and editing.

**Funding** Open access funding provided by University of the Witwatersrand. The authors declare that there is no funding involved in this research.

**Data Availability** Rainfall data sets are available upon request at https://www.weathersa.co.za/home/equiries_climatedata, while discharge datasets can be downloaded from https://www.dws.gov.za/Hydrology/Verified/hymain.aspx. The CMIP5 data was downloaded from the Earth System Grid Federation (ESGF) platform (https://esgf-node.llnl.gov/projects/esgf-llnl/). Data sets generated during the current study are available from the corresponding author on reasonable request.

**Declaration**

**Conflict of interest** On behalf of all authors, there is no conflict of interest to declare.

**Ethical approval** This article does not involve human or animal subjects.



## References

Abiodun BJ, Abba Omar S, Lennard C, Jack C (2016) Using regional climate models to simulate extreme rainfall events in the Western Cape, South Africa: Simulating extreme rainfall events in Western Cape. Int J Climatol 36:689–705. https://doi.org/10.1002/joc.4376

Abiodun BJ, Mogebisa TO, Petja B et al (2020) Potential impacts of specific global warming levels on extreme rainfall events over southern Africa in CORDEX and NEX-GDDP ensembles. Int J Climatol 40:3118–3141. https://doi.org/10.1002/joc.6386

Almasi P, Soltani S (2017) Assessment of the climate change impacts on flood frequency (case study: Bazoft Basin, Iran). Stoch Environ Res Risk Assess 31:1171–1182. https://doi.org/10.1007/s00477-016-1263-1

Andersson L, Samuelsson P, Kjellström E (2011) Assessment of climate change impact on water resources in the Pungwe river basin. Tellus a: Dyn Meteorol Oceanogr 63:138–157. https://doi.org/10.1111/j.1600-0870.2010.00480.x

Arnell N (1999) Climate change and global water resources. Glob Environ Chang 9:S31–S49. https://doi.org/10.1016/S0959-3780(99)00017-5

Arnell NW, Gosling SN (2013) The impacts of climate change on river flow regimes at the global scale. J Hydrol 486:351–364. https://doi.org/10.1016/j.jhydrol.2013.02.010

Arnell NW, Hudson DA, Jones RG (2003) Climate change scenarios from a regional climate model: Estimating change in runoff in southern Africa. J Geophys Res Atmos 108:1–17. https://doi.org/10.1029/2002JD002782

Bailey AK, Pitman WV (2016) Water Resources of South Africa 2012 Study (WR2012) Volume 7: WRSM/Pitman User Manual. Water Resources Commission, South Africa

Bannister D, Herzog M, Graf H-F et al (2017) An assessment of recent and future temperature change over the Sichuan basin, China, using CMIP5 climate models. J Clim 30:6701–6722. https://doi.org/10.1175/JCLI-D-16-0536.1

Brönnimann S, Frigerio L, Schwander M et al (2019) Causes of increased flood frequency in central Europe in the 19th century. Clim past 15:1395–1409. https://doi.org/10.5194/cp-15-1395-2019

Bulti DT, Abebe BG, Biru Z (2021) Analysis of the changes in historical and future extreme precipitation under climate change in Adama city, Ethiopia. Model Earth Syst Environ 7:2575–2587. https://doi.org/10.1007/s40808-020-01019-x

Camici S, Brocca L, Melone F, Moramarco T (2014) Impact of climate change on flood frequency using different climate models and downscaling approaches. J Hydrol Eng 19:04014002. https://doi.org/10.1061/(ASCE)HE.1943-5584.0000959

Cannon AJ, Sobie SR, Murdock TQ (2015) Bias correction of GCM precipitation by quantile mapping: How well do methods

preserve changes in quantiles and extremes? J Clim 28:6938–6959. https://doi.org/10.1175/JCLI-D-14-00754.1
Centre for Environmental Data Analysis (CEDA) (2024) The CEDA archive. Centre for Environmental Data Analysis, Didcot, United Kingdom. https://catalogue.ceda.ac.uk/
Centre for Research on the Epidemiology of Disasters (CRED) (2023) The international disaster database. Centre for Research on the Epidemiology of Disasters, Brussels, Belgium
Chen J, Brissette FP, Poulin A, Leconte R (2011) Overall uncertainty study of the hydrological impacts of climate change for a Canadian watershed. Water Resour Res. https://doi.org/10.1029/2011WR010602
Chen B, Krajewski WF, Liu F et al (2017) Estimating instantaneous peak flow from mean daily flow. Hydrol Res 48:1474–1488. https://doi.org/10.2166/nh.2017.200
Chokkavarapu N, Mandla VR (2019) Comparative study of GCMs, RCMs, downscaling and hydrological models: a review toward future climate change impact estimation. SN Appl Sci 1:1698. https://doi.org/10.1007/s42452-019-1764-x
Chow VT (1954) Discussion of "the log-probability law and Its engineering applications." J Hydraul Div. https://doi.org/10.1061/JYCEAJ.0000005
Copernicus Climate Change Service (2021) What is statistical and dynamical downscaling? https://climate.copernicus.eu/sites/default/files/2021-01/infosheet8.pdf
Cordery I, Fraser J (2000) Characteristics of rainfall and transmission losses in the Australian arid zone. New Delhi, India, pp 611–616
Cullis J, Alton T, Arndt C, et al (2015) An uncertainty approach to modelling climate change risk in South Africa. Wider Working Paper. United Nations University, pp 1–122. https://www.wider.unu.edu/sites/default/files/WP2015-045-.pdf
Cunnane C (1988) Methods and merits of regional flood frequency analysis. J Hydrol 100:269–290. https://doi.org/10.1016/0022-1694(88)90188-6
Davis C, Archer E, Engelbrecht F, Landman W, et al (2010) A climate change handbook for North-Eastern South Africa. CSIR Pretoria South Africa https://ees.kuleuven.be/eng/klimos/toolkit/documents/317_cc_handbook_sa.pdf
De Waal JH, Chapman A, Kemp J (2017) Extreme 1-day rainfall distributions: analysing change in the Western Cape. South Afr J Sci 113:8. https://doi.org/10.17159/sajs.2017/20160301
Dedekind Z, Engelbrecht FA, Van Der Merwe J (2016) Model simulations of rainfall over southern Africa and its eastern escarpment. Water SA 42:129. https://doi.org/10.4314/wsa.v42i1.13
der Spuy V, du Plessis (2022) Flood frequency analysis—Part 1: review of the statistical approach in South Africa. Water SA. https://doi.org/10.17159/wsa/2022.v48.i2.3848.1
Dobler C, Hagemann S, Wilby RL, Stötter J (2012) Quantifying different sources of uncertainty in hydrological projections in an Alpine watershed. Hydrol Earth Syst Sci 16:4343–4360. https://doi.org/10.5194/hess-16-4343-2012
Dong ND, Jayakumar KV, Agilan V (2018) Impact of climate change on flood frequency of the Trian reservoir in Vietnam Using RCMS. J Hydrol Eng 23:05017032. https://doi.org/10.1061/(ASCE)HE.1943-5584.0001609
Du Plessis JA, Kalima SG (2021) Modelling the impact of climate change on the flow of the Eerste River in South Africa. Phys Chem Earth, Parts a/b/c 124:1–13. https://doi.org/10.1016/j.pce.2021.103025
du Plessis J, Schloms B (2017) An investigation into the evidence of seasonal rainfall pattern shifts in the Western Cape, South Africa. J South Afr Inst Civ Eng 59:47–55. https://doi.org/10.17159/2309-8775/2017/v59n4a5
Edokpayi JN, Makungo R, Mathivha F, et al (2020) Influence of global climate change on water resources in South Africa: toward an adaptive management approach. In: Water conservation and wastewater treatment in BRICS nations, Elsevier: Amsterdam. https://doi.org/10.1016/B978-0-12-818339-7.00005-9
Engelbrecht CJ, Engelbrecht FA, Dyson LL (2013) High-resolution model-projected changes in mid-tropospheric closed-lows and extreme rainfall events over southern Africa. Int J Climatol 33:173–187. https://doi.org/10.1002/joc.3420
Engelbrecht F (2019) Detailed projections of future climate change over South Africa. Council for Scientific and Industrial Research (CSIR), Pretoria, South Africa
Fan X, Jiang L, Gou J (2021) Statistical downscaling and projection of future temperatures across the Loess Plateau, China. Weather Clim Extrem 32:100328. https://doi.org/10.1016/j.wace.2021.100328
Farquharson FAK, Meigh JR, Sutcliffe JV (1992) Regional flood frequency analysis in arid and semi-arid areas. J Hydrol 138:487–501. https://doi.org/10.1016/0022-1694(92)90132-F
Fikileni S, Wolski P (2022) Framework for implementation of the Pitman-WR2012 model in seasonal hydrological forecasting: a case study of Kraai River South Africa. Water SA. https://doi.org/10.17159/wsa/2022.v48.i1.3891
Fuller WE (1914) Flood flows. Trans Am Soc Civ Eng 77:564–617. https://doi.org/10.1061/taceat.0002552
Giuntoli I, Prosdocimi I, Hannah DM (2021) Going beyond the ensemble mean: assessment of future floods from global multimodels. Water Resour Res 57:e2020WR027897. https://doi.org/10.1029/2020WR027897
Gupta HV, Kling H, Yilmaz KK, Martinez GF (2009) Decomposition of the mean squared error and NSE performance criteria: implications for improving hydrological modelling. J Hydrol 377:80–91. https://doi.org/10.1016/j.jhydrol.2009.08.003
Hawkins E, Sutton R (2011) The potential to narrow uncertainty in projections of regional precipitation change. Clim Dyn 37:407–418. https://doi.org/10.1007/s00382-010-0810-6
Heritage GL, Moon BP, Jewitt GP et al (2001) The February 2000 floods on the Sabie River, South Africa: an examination of their magnitude and frequency. Koedoe 44:37–44. https://doi.org/10.4102/koedoe.v44i1.184
Hewitson BC, Crane RG (2006) Consensus between GCM climate change projections with empirical downscaling: precipitation downscaling over South Africa. Int J Climatol 26:1315–1337. https://doi.org/10.1002/joc.1314
Hosking JRM, Wallis JR (1997) Regional frequency analysis: An approach based on L-moments, 1st edn. Cambridge, Cambridge University Press
Hughes DA, Mantel S, Mohobane T (2014) An assessment of the skill of downscaled GCM outputs in simulating historical patterns of rainfall variability in South Africa. Hydrol Res 45:134–147. https://doi.org/10.2166/nh.2013.027
Iqbal M, Dahri Z, Querner E et al (2018) Impact of climate change on flood frequency and intensity in the Kabul River basin. Geosciences 8:114. https://doi.org/10.3390/geosciences8040114
Jimeno-Sáez P, Senent-Aparicio J, Pérez-Sánchez J et al (2017) Estimation of instantaneous peak flow using machine-learning models and empirical formula in Peninsular Spain. Water 9:1–12. https://doi.org/10.3390/w9050347
Jose DM, Vincent AM, Dwarakish GS (2022) Improving multiple model ensemble predictions of daily precipitation and temperature through machine learning techniques. Sci Rep 12:4678. https://doi.org/10.1038/s41598-022-08786-w
Kay AL, Jones RG, Reynard NS (2006) RCM rainfall for UK flood frequency estimation. II. Climate Change Results J Hydrol 318:163–172. https://doi.org/10.1016/j.jhydrol.2005.06.013
Kay AL, Davies HN, Bell VA, Jones RG (2009) Comparison of uncertainty sources for climate change impacts: flood

frequency in England. Clim Change 92:41–63. https://doi.org/10.1007/s10584-008-9471-4
Khazaei MR, Zahabiyoun B, Saghafian B (2012) Assessment of climate change impact on floods using weather generator and continuous rainfall-runoff model. Int J Climatol 32:1997–2006. https://doi.org/10.1002/joc.2416
Kim Y, Kwon H, Lima C, Sharma A (2021) A novel spatial downscaling approach for climate change assessment in regions with sparse ground data networks. Geophys Res Lett. https://doi.org/10.1029/2021GL095729
Kjeldsen TR, Smithers JC, Schulze RE (2002) Regional flood frequency analysis in the KwaZulu-Natal province, South Africa, using the index-flood method. J Hydrol 255:194–211. https://doi.org/10.1016/S0022-1694(01)00520-0
Kjeldsen TR, Macdonald N, Lang M et al (2014) Documentary evidence of past floods in Europe and their utility in flood frequency estimation. J Hydrol 517:963–973. https://doi.org/10.1016/j.jhydrol.2014.06.038
Kling H, Fuchs M, Paulin M (2012) Runoff conditions in the upper Danube basin under an ensemble of climate change scenarios. J Hydrol 424–425:264–277. https://doi.org/10.1016/j.jhydrol.2012.01.011
Kruger AC, Nxumalo MP (2017) Historical rainfall trends in South Africa: 1921–2015. Water SA 43:285. https://doi.org/10.4314/wsa.v43i2.12
Lakhraj-Govender R, Grab SW (2019) Rainfall and river flow trends for the Western Cape Province South Africa. South Afr J Sci. https://doi.org/10.17159/sajs.2019/6028
Langbein WB (1949) Annual floods and the partial-duration flood series. Trans Am Geophys Union 30:879. https://doi.org/10.1029/TR030i006p00879
Lee J, Lee JE, Kim NW (2020) Estimation of hourly flood hydrograph from daily flows using artificial neural network and flow disaggregation technique. Water 13:1–16. https://doi.org/10.3390/w13010030
Leščešen I, Urošev M, Dolinaj D et al (2019) Regional flood frequency analysis based on L-moment approach (case study Tisza River basin). Water Resour 46:853–860. https://doi.org/10.1134/S0097807819060006X
Lin F, Chen X, Yao H (2017) Evaluating the use of nash-sutcliffe efficiency coefficient in goodness-of-fit measures for daily runoff simulation with SWAT. J Hydrol Eng 22:05017023. https://doi.org/10.1061/(ASCE)HE.1943-5584.0001580
Liu D (2020) A rational performance criterion for hydrological model. J Hydrol 590:125488. https://doi.org/10.1016/j.jhydrol.2020.125488
Loyeh NS, Bavani AM (2021) Daily maximum runoff frequency analysis under non-stationary conditions due to climate change in the future period: case study Ghareh Sou basin. J Water Clim Change 12:1910–1929. https://doi.org/10.2166/wcc.2021.074
MacKellar N, New M, Jack C (2014) Observed and modelled trends in rainfall and temperature for South Africa: 1960–2010. South Afr J Sci 110:13. https://doi.org/10.1590/sajs.2014/20130353
Maghsood FF, Moradi H, Massah Bavani AR et al (2019) Climate change impact on flood frequency and source area in Northern Iran under CMIP5 Scenarios. Water 11:1–21. https://doi.org/10.3390/w11020273
Maimone M, Malter S, Rockwell J, Raj V (2019) Transforming global climate model precipitation output for use in urban stormwater applications. J Water Resour Plan Manag 145:04019021. https://doi.org/10.1061/(ASCE)WR.1943-5452.0001071
Mareuil A, Leconte R, Brissette F, Minville M (2007) Impacts of climate change on the frequency and severity of floods in the Châteauguay River basin, Canada. Can J Civ Eng 34:1048–1060. https://doi.org/10.1139/l07-022
Markiewicz I, Strupczewski WG, Bogdanowicz E, Kochanek K (2015) Generalized exponential distribution in flood frequency analysis for Polish rivers. PLoS ONE 10:e0143965. https://doi.org/10.1371/journal.pone.0143965
Mason SJ, Joubert AM (1997) Simulated changes in extreme rainfall over southern Africa. Int J Climatol 17:291–301
Maurer EP, Kayser G, Doyle L, Wood AW (2018) Adjusting flood peak frequency changes to account for climate change impacts in the Western United States. J Water Resour Plan Manag 144:05017025. https://doi.org/10.1061/(ASCE)WR.1943-5452.0000903
Mazibuko SM, Mukwada G, Moeletsi ME (2021) Assessing the frequency of drought/flood severity in the Luvuvhu River catchment, Limpopo Province, South Africa. Water SA 47:172–184. https://doi.org/10.17159/wsa/2021.v47.i2.10913
Mendoza PA, Clark MP, Mizukami N et al (2015) Effects of hydrologic model choice and calibration on the portrayal of climate change impacts. J Hydrometeorol 16:762–780. https://doi.org/10.1175/JHM-D-14-0104.1
Miao C, Duan Q, Sun Q et al (2014) Assessment of CMIP5 climate models and projected temperature changes over Northern Eurasia. Environ Res Lett 9:055007. https://doi.org/10.1088/1748-9326/9/5/055007
Mizukami N, Clark MP, Gutmann ED et al (2016) Implications of the methodological choices for hydrologic portrayals of climate change over the contiguous United States: Statistically downscaled forcing data and hydrologic models. J Hydrometeorol 17:73–98. https://doi.org/10.1175/JHM-D-14-0187.1
Moritz S (2017) How to deal with missing data in time series and the imputeTS package. https://rmisstastic.netlify.app/tutorials/Moritz_slides_TimeSeries_2017.pdf
Muzik I (2002) A first-order analysis of the climate change effect on flood frequencies in a subalpine watershed by means of a hydrological rainfall–runoff model. J Hydrol 267:65–73. https://doi.org/10.1016/S0022-1694(02)00140-3
Nagy BK, Mohssen M, Hughey KFD (2017) Flood frequency analysis for a braided river catchment in New Zealand: comparing annual maximum and partial duration series with varying record lengths. J Hydrol 547:365–374. https://doi.org/10.1016/j.jhydrol.2017.02.001
Najafi MR, Moradkhani H, Jung IW (2011) Assessing the uncertainties of hydrologic model selection in climate change impact studies. Hydrol Process 25:2814–2826. https://doi.org/10.1002/hyp.8043
Nathanael J, Smithers J, Horan M (2018) Assessing the performance of regional flood frequency analysis methods in South Africa. Water SA. https://doi.org/10.4314/wsa.v44i3.06
Ndebele NE, Grab S, Turasie A (2020) Characterizing rainfall in the south-western Cape, South Africa: 1841–2016. Int J Climatol 40:1992–2014. https://doi.org/10.1002/joc.6314
Ndebele NE, Grab S, Hove H (2022) Wet season rainfall characteristics and temporal changes for Cape Town, South Africa, 1841–2018. Clim past 18:2463–2482. https://doi.org/10.5194/cp-18-2463-2022
Ngongondo C, Xu C-Y, Gottschalk L, Alemaw B (2011) Evaluation of spatial and temporal characteristics of rainfall in Malawi: a case of data scarce region. Theor Appl Climatol 106:79–93. https://doi.org/10.1007/s00704-011-0413-0
Ngongondo C, Li L, Gong L et al (2013) Flood frequency under changing climate in the upper Kafue River basin, southern Africa: a large-scale hydrological model application. Stoch Environ Res Risk Assess 27:1883–1898. https://doi.org/10.1007/s00477-013-0724-z
Ngwenya M, Simatele MD (2024) Modeling future (2021–2050) meteorological drought characteristics using CMIP6 climate scenarios in the Western Cape Province, South Africa. Modeling

Earth Syst Environ 10:2957–2975. https://doi.org/10.1007/s40808-023-01937-6
Ougahi JH, Karim S, Mahmood SA (2022) Application of the SWAT model to assess climate and land use/cover change impacts on water balance components of the Kabul River Basin, Afghanistan. J Water Clim Change 13:3977–3999. https://doi.org/10.2166/wcc.2022.261
Parding KM, Dobler A, McSweeney CF et al (2020) GCMeval—An interactive tool for evaluation and selection of climate model ensembles. Clim Serv 18:100167. https://doi.org/10.1016/j.cliser.2020.100167
Pascale S, Lucarini V, Feng X et al (2016) Projected changes of rainfall seasonality and dry spells in a high greenhouse gas emissions scenario. Clim Dyn 46:1331–1350. https://doi.org/10.1007/s00382-015-2648-4
Pharoah R, Holloway A, Fortune G, et al (2016) Off the radar—synthesis report. High impact weather events in the Western Cape, South Africa 2003–2014. Research Alliance for Disaster and Risk Reduction, Department of Geography and Environmental Studies, Stellenbosch, Western Cape
Pillay K (2023) Assessing changes in flood frequency using the partial duration series under future climate change in the Western Cape, South Africa. Forthcoming pp 1–26
Pitman WV (1976) A mathematical model for generating daily flows from meteorological data in South Africa. University of Witwatersrand, Johannesburg, South Africa
Pitman WV, Bailey AK (2021) Can CHIRPS fill the gap left by the decline in the availability of rainfall stations in Southern Africa? Water SA. https://doi.org/10.17159/wsa/2021.v47.i2.10912
Qin XS, Lu Y (2014) Study of climate change impact on flood frequencies: a combined weather generator and hydrological modeling approach. J Hydrometeorol 15:1205–1219. https://doi.org/10.1175/JHM-D-13-0126.1
Quintero F, Mantilla R, Anderson C et al (2018) Assessment of changes in flood frequency due to the effects of climate change: implications for engineering design. Hydrology 5:19. https://doi.org/10.3390/hydrology5010019
Reinwarth B, Riddell ES, Glotzbach C, Baade J (2018) Estimating the sediment trap efficiency of intermittently dry reservoirs: lessons from the Kruger National Park, South Africa. Earth Surf Process Landf 43:463–481. https://doi.org/10.1002/esp.4263
Roffe SJ, Fitchett JM, Curtis CJ (2019) Classifying and mapping rainfall seasonality in South Africa: a review. South Afr Geogr J 101:158–174. https://doi.org/10.1080/03736245.2019.1573151
Roffe SJ, Fitchett JM, Curtis CJ (2021) Investigating changes in rainfall seasonality across South Africa: 1987–2016. Int J Climatol 41:E2031–E2050. https://doi.org/10.1002/joc.6830
Sangal BP (1983) Practical method of estimating peak flow. J Hydraul Eng 109:549–563. https://doi.org/10.1061/(ASCE)0733-9429(1983)109:4(549)
Seidou O, Ramsay A, Nistor I (2012) Climate change impacts on extreme floods II: improving flood future peaks simulation using non-stationary frequency analysis. Nat Hazards 60:715–726. https://doi.org/10.1007/s11069-011-0047-7
Shaw SB, Riha SJ (2011) Assessing possible changes in flood frequency due to climate change in mid-sized watersheds in New York State, USA. Hydrol Process 25:2542–2550. https://doi.org/10.1002/hyp.8027
Singo LR, Kundu PM, Mathivha FI, Odiyo JO (2016) Evaluation of flood risks using flood frequency models: a case study of Luvuvhu River Catchment in Limpopo Province, South Africa. Venice, Italy, pp 215–226
Smithers J (2012) Methods for design flood estimation in South Africa. Water SA 38:633–646. https://doi.org/10.4314/wsa.v38i4.19
Smithers J, Schulze R (2004) The estimation of design rainfalls for South Africa using a regional scale invariant approach. Water SA 30:435–444. https://doi.org/10.4314/wsa.v30i4.5095
Smithers J, Streatfield J, Gray R, Oakes E (2015) Performance of regional flood frequency analysis methods in KwaZulu-Natal, South Africa. Water SA 41:390. https://doi.org/10.4314/wsa.v41i3.11
Soriano E, Mediero L, Garijo C (2019) Selection of bias correction methods to assess the impact of climate change on flood frequency curves. Water 11:2266. https://doi.org/10.3390/w11112266
Stergiou I, Tagaris E, Sotiropoulou R-EP (2021) Investigating the WRF temperature and precipitation performance sensitivity to spatial resolution over central Europe. Atmosphere 12:278. https://doi.org/10.3390/atmos12020278
Tabari H, Paz SM, Buekenhout D, Willems P (2021) Comparison of statistical downscaling methods for climate change impact analysis on precipitation-driven drought. Hydrol Earth Syst Sci 25:3493–3517. https://doi.org/10.5194/hess-25-3493-2021
Tempelhoff J, Van Niekerk D, Van Eeden E et al (2009) The December 2004–January 2005 floods in the Garden Route region of the Southern Cape, South Africa. Jàmbá J Disaster Risk Stud 2:93–112. https://doi.org/10.4102/jamba.v2i2.18
Watson A, Midgley G, Künne A, Kralisch S et al (2021) Determining hydrological variability using a multi-catchment model approach for the Western Cape. South Afr Sustain 13:14058. https://doi.org/10.3390/su132414058
Western Cape Government (2018) Western Cape sustainable water management Plan 2017–2022. Western Cape Government, Western Cape
Westra S, Alexander LV, Zwiers FW (2013) Global increasing trends in annual maximum daily precipitation. J Clim 26:3904–3918. https://doi.org/10.1175/JCLI-D-12-00502.1
World Bank Group (2021) Climate Risk Country Profile: South Africa. World Bank Group
Xavier ACF, Martins LL, Rudke AP et al (2022) Evaluation of Quantile Delta Mapping as a bias-correction method in maximum rainfall dataset from downscaled models in São Paulo state (Brazil). Int J Climatol 42:175–190. https://doi.org/10.1002/joc.7238
Xu C, Widén E, Halldin S (2005) Modelling hydrological consequences of climate change—Progress and challenges. Adv Atmospheric Sci 22:789–797. https://doi.org/10.1007/BF02918679
Zaman MA, Rahman A, Haddad K (2012) Regional flood frequency analysis in arid regions: a case study for Australia. J Hydrol 475:74–83. https://doi.org/10.1016/j.jhydrol.2012.08.054